DIFFUSION TENSOR IMAGING ANALYSIS FOR SUBCONCUSSIVE TRAUMA

IN FOOTBALL AND CONVOLUTIONAL NEURAL NETWORK-BASED

IMAGE QUALITY CONTROL THAT DOES NOT REQUIRE A BIG DATASET

A Dissertation

Submitted to the Faculty

of

Purdue University

by

Ikbeom Jang

In Partial Fulfillment of the

Requirements for the Degree

of

Doctor of Philosophy

May 2019

Purdue University

West Lafayette, Indiana

THE PURDUE UNIVERSITY GRADUATE SCHOOL
STATEMENT OF DISSERTATION APPROVAL

Dr. Thomas M. Talavage, Chair

    School of Electrical and Computer Engineering

Dr. Eric A. Nauman

    School of Mechanical Engineering

Dr. Edward J. Delp

    School of Electrical and Computer Engineering

Dr. Michael D. Zoltowski

    School of Electrical and Computer Engineering

Approved by:

    Dr. Pedro Irazoqui

        Head of the School Graduate Program

For my family and my parents

ACKNOWLEDGMENTS

I would like to express my sincere gratitude to my advisor Prof. Thomas Talavage for allowing me to explore my interests and for his continuous support and advice. His guidance helped me in all the time of research and writing of this dissertation.

Special thanks to Prof. Anne Sereno and Prof. Yunjie Tong for providing opportunities to explore various projects in the field of neuroscience and for their continued support and advice.

To my fellow colleagues Victoria Poole, Il Yong Chun, Trey Shenk, and Kausar Abbas for all of the guidance and advice in my early days. To Sumra Bari, Yukai Zou, Andres Llico, Pratik Kashap, Nicole Vike, Taylor Lee, Diana Svaldi, Xianglun Mao, Minseok Kwon, Allan Diaz, and Chetas Joshi for being the people I could always discuss research with as well as for our lasting friendships.

To my committee members, Prof. Eric Nauman, Prof. Edward Delp, and Prof. Michael Zoltowski for their insightful comments and encouragement.

Last but not the least, my sincere thanks go to my wife Ji Yoon Jung for always being the person I could turn to and for continuous encouragement throughout my years of study. To my little girl Evelyn for being healthy, sleeping well at night, and being my daughter. To my parents for supporting me spiritually throughout my life.

TABLE OF CONTENTS

LIST OF TABLES

LIST OF FIGURES

ABBREVIATIONS

AD	Axial diffusivity
CI	Confidence interval
CNN	Convolutional neural network
CT	Computed tomography
CTE	Chronic traumatic encephalopathy
DCNN	Deep convolutional neural network
DICOM	Digital imaging and communications in medicine
DTI	Diffusion tensor imaging
DWI	Diffusion-weighted imaging
FA	Fractional anisotropy
FBA	Football athletes
fMRI	Functional magnetic resonance imaging
GPU	Graphics processing unit
HAE	Head acceleration event
MD	Mean diffusivity
MRI	Magnetic resonance imaging
mTBI	Mild traumatic brain injury
NCA	Non-collision athletes
PNG	Purdue Neurotrauma Group
QA	Quality assessment
QC	Quality control
RD	Radial diffusivity
ROC	Receiver-operating characteristic
ROI	Region of interest

SNR Signal-to-noise ratio

TBI Traumatic brain injury

WM White matter

ABSTRACT

Jang, Ikbeom Ph.D., Purdue University, May 2019. Diffusion Tensor Imaging Analysis for Subconcussive Trauma in Football and Convolutional Neural Network-Based Image Quality Control That Does Not Require a Big Dataset. Major Professor: Thomas M. Talavage.

Diffusion Tensor Imaging (DTI) is a magnetic resonance imaging (MRI)-based technique that has frequently been used for the identification of brain biomarkers of neurodevelopmental and neurodegenerative disorders because of its ability to assess the structural organization of brain tissue. In this work, I present (1) preclinical findings of a longitudinal DTI study that investigated asymptomatic high school football athletes who experienced repetitive head impact and (2) an automated pipeline for assessing the quality of DTI images that uses a convolutional neural network (CNN) and transfer learning. The first section addresses the effects of repetitive subconcussive head trauma on the white matter of adolescent brains. Significant concerns exist regarding sub-concussive injury in football since many studies have reported that repetitive blows to the head may change the microstructure of white matter. This is more problematic in youth-aged athletes whose white matter is still developing. Using DTI and head impact monitoring sensors, regions of significantly altered white matter were identified and within-season effects of impact exposure were characterized by identifying the volume of regions showing significant changes for each individual. The second section presents a novel pipeline for DTI quality control (QC). The complex nature and long acquisition time associated with DTI make it susceptible to artifacts that often result in inferior diagnostic image quality. We propose an automated QC algorithm based on a deep convolutional neural network (DCNN). Adaptation of transfer learning makes it possible to train a DCNN with a relatively small dataset in a short time. The QA algorithm detects not only motion- or gradient-related ar-

tifacts, but also various erroneous acquisitions, including images with regional signal loss or those that have been incorrectly imaged or reconstructed.

1. INTRODUCTION

1.1 Neurotrauma Study Using Diffusion Tensor Imaging

This work is part of the larger Purdue Neurotrauma Group (PNG) study, which aims to examine the connection between mild traumatic brain injury (mTBI) biomechanics and the underlying pathophysiology as well as methods for the prevention of mTBI, especially in the context of youth athletics. The long-term goal of PNG is to ensure that youths can more safely participate in collision-based sports (e.g., American football, soccer).

In 2017, 2.5-million high school students in the United States reported having at least one sport-related concussion and 1-million reported having more than one concussion in that year [1]. However, the underlying mechanism that governs the development of sports-related concussions or the effects of accumulated subconcussive head impacts are largely unknown. A major cause for concern is that approximately half of all concussions go undiagnosed [2–4] and failure to identify a concussion or any form of damage may result in long-term neurodegeneration [5–8]. Multiple on-site healthcare professionals are present at games and practices to watch for symptoms of concussion following any severe collisions. Commonly identified signs are somatic symptoms such as headache, feeling dazed, and emotional instability; physical signs such as loss of consciousness or amnesia; balance impairment; behavioral changes; cognitive impairment; and sleep-wake disturbance [9]. However, symptoms may not present or may not be noticed right after trauma [10] and damage may accumulate over time [11]. The standard-of-care diagnostic procedures associated with mTBI or concussion often fail to identify certain forms of damage; additionally, a set of biomarkers for predicting long-term damage or recovery has yet to be established.

Furthermore, impacts that do not immediately cause symptoms of a concussion (termed subconcussive head impact exposures) can alter neural integrity. Because these incidents do not elicit identifiable symptoms, athletes continue to participate with unclear consequences. Neuroimaging studies have found that neurological changes are associated with repetitive head impact exposures, including alterations of functional connectivity in gray matter [12–15], microstructural changes in white matter [16–20], and increased susceptibility to concussion [10, 21, 22]. Studies have also revealed that, in the long-term, retired football athletes who were exposed to a massive number of subconcussive impacts tend to have a higher risk of developing neurodegenerative disorders such as chronic traumatic encephalopathy (CTE), Alzheimers disease, and Parkinsons disease [7, 8, 11, 23, 24].

This work focuses on clinically asymptomatic high school football athletes, since football accounts for a large proportion of sports-related concussions [25]. I use diffusion-weighted imaging (DWI) data acquired in our prospective study of high school-aged American football athletes to identify the nature and extent of the structural changes in white matter associated with the accumulation of exposure to head acceleration events (HAEs). Diffusion tensor imaging (DTI) data are acquired by processing DWI data. Compared to other neuroimaging methods, DTI is known to be more sensitive to subtle changes in white matter integrity. DTI provides directional and diffusivity information of water molecules at each voxel in endogenous tissue. The two major estimates most commonly used in DTI studies are fractional anisotropy (FA) and mean diffusivity (MD), where FA represents coherence of fibers and MD quantifies averaged diffusivity. To assess relative mechanical loading, HAEs were monitored using telemetry systems equipped with accelerometer and gyroscope sensors. Athletes were monitored throughout all team practices and games. An important advantage of this work and of the PNG study is the availability of longitudinal measurements, including baseline data, which are acquired prior to the start of the playing season. This benefit offers the rare opportunity to monitor changes in individuals during and after a football season.

While many TBI studies adopt region of interest (ROI)-based analysis in which measurements taken from regions of interest or throughout the whole brain are averaged, this may not provide sufficient information concerning the structure of white matter since the measurements of each voxel do not necessarily react to HAEs in the same manner across different locations. As such, this study focuses more on voxel-level analyses. Starting from more basic analyses such as comparisons of FA and MD at the whole brain level, the group-level regions of alteration was identified relative to the baseline through voxel-wise comparisons, and the individual-level extent of alteration was found at each follow-up imaging session, which was then passed to regression analyses to investigate the effects of cumulative HAE exposure. These in-depth analyses allowed deeper understanding of mechanisms of longitudinal white matter changes due to repetitive subconcussive trauma.

1.2 Automated Quality Control of Diffusion Tensor Imaging

DTI is a well-established and powerful technique that can non-invasively probe the composition, integrity, and orientation of white matter fibers in the brain [26, 27] . Due to inherent limitations of acquisition, however, DTI suffers from artifacts introduced by motion (e.g., body movement, cardiac pulsation), eddy currents, and susceptibility effects [27]. DTI further suffers from a relatively low signal-to-noise ratio (SNR), which hinders accurate estimation of diffusion parameters, interpretation, and reproducibility [28, 29].

For application of DTI analysis to large-scale studies particularly those involving longitudinal assessment of DTI quality control (QC) or quality assessment (QA) are critical. Many QC approaches focus on reducing specific artifacts, including geometric distortion artifacts induced by the combination of eddy currents [30] and motion [28, 31], and general noise reduction [29]. These approaches have been applied to both the acquisition and post-processing stages [28]. Given the number of correction stages in a typical DTI processing pipeline, and the large number of slices associated

with an acquisition, it is desirable to have an automated QC process. Several tools are presently available for this [31–34]; however, in practice, these tools require significant effort on part of investigators.

One approach for developing an automated QA process for a large number of images would be to use a supervised learning approach based on machine learning [35, 36] or deep learning algorithms, such as a convolutional neural network (CNN) [37]. A CNN is a class of deep neural network, which has been successfully used in various computer vision problems such as object detection, image segmentation, and video classification. A CNN that contains many layers is referred to as a deep CNN (DCNN). While offering high classification accuracy, DCNNs can be time-consuming and are expensive to train (possibly several weeks, even with a high-performance GPU); thus, Transfer Learning [38] is often used to reduce learning time through use of weights from a network that was trained for a different, but related, domain or task.

I present a QC algorithm based on a DCNN transferred from a heterogeneous domain, which enables fully automated QC of DTI. Base networks used for transfer learning are Inception-ResNet-v2, Inception-v3, ResNet-50, and VGG-19. More conventional algorithms (e.g., support vector machine, random forest) are also considered for comparison. I evaluate the performance of these models and provide a receiver-operating characteristic (ROC) that can enable users to determine a task specific threshold to optimize performance. The strengths of the proposed method include high detection accuracy, the ability to detect numerous types of artifacts, and the ability to be customized and generalized.

2. WHITE MATTER DIFFUSIVITY CHANGES IN HIGH SCHOOL ATHLETES ARE CORRELATED WITH REPETITIVE HEAD ACCELERATION EVENT EXPOSURE

2.1 Abstract

Recent evidence of short-term alterations in brain physiology associated with repeated exposure to moderate intensity subconcussive head acceleration events (HAEs), prompts the question whether these alterations represent an underlying neural injury. A retrospective analysis combining counts of experienced HAEs and longitudinal diffusion-weighted imaging (DWI) explored whether greater exposure to incident mechanical forces was associated with traditional DWI measures of neural injury— reduced fractional anisotropy (FA) and increased mean diffusivity (MD). Brains of high school athletes (N=61) participating in American football exhibited greater volumes experiencing significant changes (increases and decreases) in both FA and MD than brains of peers who do not participate in collision-based sports (N=15). Further, the football athlete brain volumes exhibiting traditional DWI markers of neural injury were found to be significantly correlated with the cumulative exposure to HAEs having peak translational acceleration exceeding $20g$. This finding demonstrates that subconcussive HAEs induce low-level neurotrauma, with prolonged exposure producing greater accumulation of neuronal damage. The duration and extent of recovery associated with periods in which athletes do not experience subconcussive HAEs now represents a priority for future study, such that appropriate participation and training schedules may be developed to minimize the risk of long-term neurological dysfunction.

2.2   Keywords

Subconcussive Injury; Traumatic Brain Injury; Magnetic Resonance Imaging; Diffusion Tensor Imaging; Football

2.3 Introduction

Previous neuroimaging work has demonstrated changes in brain function and chemistry to be associated with the accumulation of exposure to head acceleration events (HAEs), even in the absence of a diagnosis of concussion. Exposure to these "subconcussive" HAEs has been observed to be associated with alterations in the brain's response to task demands [13, 39, 40], functional connectivity [12, 14, 41], cerebrovascular reactivity [15, 42, 43], biochemical concentrations [44–46], and resting perfusion [47]. Such alterations in function have been suggested as precursors to the symptoms normally resulting in the diagnosis of a concussion, with accumulation of HAEs put forth as a likely mechanism for symptom development [48].

Alterations in physiologic behavior, like those reported above, are anticipated to arise from underlying structural damage to the cells within the nervous system. Neural injury of this nature is typically assessed in MRI using diffusion-weighted imaging (DWI), with approaches focusing on white matter integrity using tensor-based analysis to achieve diffusion-tensor imaging (DTI). In DTI the diffusion of water molecules is expected to be anisotropic—specifically, stronger along the length of an axon than outward through the cellular membrane and myelin sheath. Changes in this fractional anisotropy (FA) and the associated mean diffusivity (MD) are commonly used as a method for detection or confirmation of changes to white matter health (e.g., [49–52]), but some evaluation has also been made of changes in axial diffusivity (AD) and radial diffusivity (RD) (e.g., [53–56]).

In the context of sport-related concussion and subconcussive trauma, measures of white matter health have been used to document changes associated with participation in a season of American football and soccer [16, 17, 20, 57–60]. In these studies, alterations in white matter health have been quantified through comparison of pre- and post-participation measures, with average alterations in fractional anisotropy or associated measures interpreted as evidence of the effect of the intervening (and only sometimes quantified) HAEs. However, while these studies have revealed a number of

changes in white matter health resulting from said participation, the results have been highly variable. Some studies in athletes have reported reduced FA and/or elevated MD [50,51,58,61–63] while others have provided evidence for increased FA and/or decreased MD [19,52,64–70]. While interesting, this body of findings is problematic as increases in FA and decreases in MD are typically attributed to inflammation [19,71] while decreases in FA and increases in MD are typically attributed to injury [50,72].

Therefore, the critical question whether exposure to repeated HAEs produces what would be readily recognized as "injury" to the underlying brain structure remains open. Further the literature has not effectively addressed whether these reported changes—whether linked to injury or inflammation—are predominantly driven by natural growth, participation in intensive exercise, or are direct consequences of exposure to repeated subconcussive trauma.

This retrospective study uses diffusion-weighted imaging (DWI) data acquired in our prospective study of high school-aged American football athletes to identify the nature and extent of the changes in white matter health and structure associated with the accumulation of exposure to HAEs. While assessments at the whole-brain level can reasonably be expected to reflect severe injuries, such as those associated with vehicular accidents or falls (e.g., [58,73]), the progression of damage to a symptom level likely requires a finer scale assessment. Confirmation that white matter alterations likely to reflect that one or both of inflammation or injury are correlated with known mechanical exposures will provide key insight into long-term risks associated with, but also potential short-term solutions to, accumulation of repeated subconcussive events.

2.4   Methods

2.4.1   Participants

Previously-collected data from 181 high school-aged (i.e., ages 14-18) male athletes participating in American football (N=162) or noncollision sports (N=19) were

evaluated for this study. Noncollision athletes indicated participation in track (N=9), swimming (N=6), cross-country (N=7), or basketball (N=2), with some participating in more than one sport. None of the included subjects reported having been diagnosed with a concussion within the three months prior to the period of study, nor were any diagnosed with a concussion by their team healthcare professionals during the study.

2.4.2 Participation Schedule

Football Athletes (FBA): 150 of the 162 football athletes participated in at least four MRI sessions encompassing one competition season: one acquired in the two months preceding onset of contact practices (*Pre*); one each within the first (*In1*) and second (*In2*) six-week segments of the competition season, corresponding to an average of six (*In1*) and twelve (*In2*) weeks after *Pre*; and one 4–6 months after the end of the competition season (*Post*), at an average of 34 weeks after *Pre* (see Fig. 2.1).
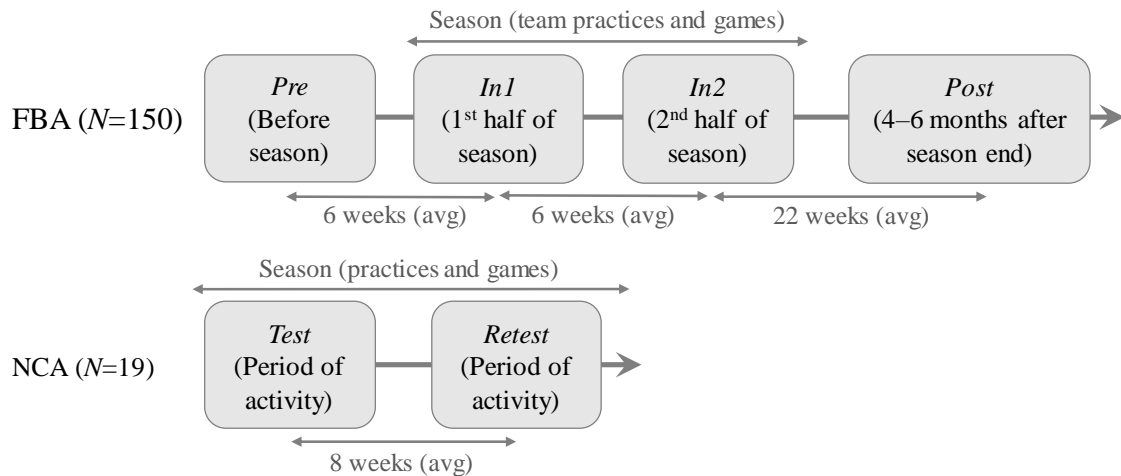
Fig. 2.1. Participation schedule for football athletes (FBA) and peer non-collision-sport athletes (NCA).

Noncollision-sport Athletes (NCA): The 19 noncollision-sport athletes were scanned twice (*Test* and *Retest*), at an interval of 5–18 weeks (average: eight weeks), while actively engaged in training or competition (see Fig. 2.1).

2.4.3 Head Acceleration Event Monitoring

All football athletes were monitored for head acceleration events (HAEs) to assess relative mechanical loading across the population. Athletes were monitored throughout all team practices and games—for details, see [74] and [75]. Sensors used were either the HIT System (Simbex, LLC), a helmet-based telemetry system; or the xPatch (X2 Biosystems, Inc), a head-mounted sensor.

Both devices were set to record all events exceeding $10g$, but analysis was conducted only on those events exceeding $20g$. Our previous work [76] suggests that $20g$ currently represents the lowest reasonable threshold for which the HIT System and xPatch are each reliable and consistent indicators of the presence of HAEs, as event counts exceeding this minimum threshold were found to be similar across both devices. It is critical to note that, based on laboratory testing, the (specific) magnitudes and locations provided for each HAE were not used in this work, as the errors associated with each individual measurement are substantial for these sensors [76,77]. However, given that both sensor systems have been found to be relatively unbiased on average (less than 25% error in most cases; see [76]), counts of events exceeding a given threshold may be expected to underestimate the true total of such events, but in a systematic manner over time within a population that permits regression analysis.

2.4.4 MRI Data Acquisition

All MRI sessions were performed at the Purdue MRI Facility, on a 3-T General Electric Signa HDx (Waukesha, WI), using a 16-channel brain array (Nova Medical; Wilmington, MA). Head motion was minimized with restraining foam pads. DWI

acquisitions used a two-dimensional spin-echo echo-planar imaging (EPI) sequence (repetition time [TR]=12,000, echo time [TE]=83.6ms, flip angle=90 degrees, field of view=240mm × 240mm, spatial resolution=$2.5mm \times 2.5mm$, slice thickness=2.5mm, slice gap=0mm, 46 contiguous axial slices, frequency readout=R/L) with 30 diffusion encoding directions at b=1000 s/mm^2 and one volume acquired at b=0 s/mm^2. Raw images were reconstructed by the GE machine to have resolution of 0.938mm × 0.938mm × 2.5mm (256 × 256 × 46 voxels).

2.4.5 Data Processing and Quality Assessment

Pre-Processing: DWI data were processed using FSL [78–80]. For each image, a brain mask was generated on the non-diffusion-weighted volume (i.e., b=0) by segmenting brain from non-brain tissues (*BET* [81]). Corrections were then applied for head movements and eddy current-induced distortions (*Eddy* [82]) while detecting slices with signal dropout and replacing them with Gaussian process predictions (–*repol* option in *Eddy* [83]). A dropout-slice was defined as a slice having average intensity four or more standard deviations lower than the expected intensity, based on the Gaussian Process prediction. Scalar diffusion tensor maps were then estimated by fitting the diffusion tensor model at each voxel (*FDT* [84]). Fractional anisotropy (FA) and mean diffusivity (MD) were subsequently calculated from the three primary eigenvalues.

Quality Assurance: Prior to voxel-wise analysis, quality assessment was performed on the images output from the preceding process, to ensure that acquisitions were not significantly corrupted. The following criteria for exclusion were similar to, but more stringent than, [85]. First, a computational assessment was conducted. Head movements during imaging were estimated between every consecutively-acquired diffusion angle, based on each volume's registration parameters [86]. Subjects with at least one relative displacement exceeding 2.5 mm per unit measurement time were excluded from the study. Those subjects who exceeded three standard devi-

ations in any translation/rotation along/around the x, y, or z-axis were also ruled out. Next a visual assessment was conducted, discarding any remaining data in which artifacts could be observed, or for which reconstruction had been improper. After quality assessment, the resulting dataset comprised complete sets of imaging data from 61 FBA (i.e., four valid imaging sessions) and 15 NCA (i.e., both valid imaging sessions). See Table 2.1 for demographics of participants whose data passed screening and were included in analyses.

Table 2.1.
Demographics of participants with complete set of valid imaging data.

	FBA (N=61)	NCA (N=15)
Age (years)		
Mean $\pm$ StdDev	16.6 $\pm$ 0.9	16.5 $\pm$ 1.2
[Min, Max]	[15, 18]	[14, 18]
Years of current sport (high school)		
Mean $\pm$ StdDev	2.2 $\pm$ 0.8	2.1 $\pm$ 1.0
[Min, Max]	[0, 3]	[0, 3]
Number of previously diagnosed concussions		
Mean $\pm$ StdDev	0.6 $\pm$ 1.0	0.5 $\pm$ 0.8
[Min, Max]	[0, 5]	[0, 2]
Racial and Ethnic Categories		
White	43	13
Black or African American	14	0
Hispanic or Latino	1	0
Asian	1	2
More than one	2	0

Image Registration: Datasets that passed quality assessment were input to the Tract-Based Spatial Statistics (TBSS) pipeline [87–90]. All FA images were nonlinearly registered to the 1mm isotropic FMRIB58-FA standard-space image, yielding a transformation for each subject. A mean FA image was calculated from the registered images from all subjects, and thresholded at 0.2 to create a mean white matter (WM) skeleton, ROI_{WM}. The aligned FA image of the *j-th* subject obtained at the *i-th* session was then projected onto the corresponding mean WM skeleton to form an individual- and session-specific WM FA skeleton ($\text{FA}_{\text{WM,j,i}}$). MD skeletons ($\text{MD}_{\text{WM,j,i}}$) were similarly created by applying the subject's transformation to the raw MD images followed by projection to the mean WM skeleton.

2.4.6   Analysis

A range of analyses was conducted to detect and characterize consequences of exposure to repetitive subconcussive HAEs associated with a single competition season of American football. Statistical analyses were performed using FMRIB Software Library (FSL) 5.0 and STATA 14.0 (StataCorp LP; College Station, TX).

Group-level longitudinal changes in mean FA and MD: A one-way repeated measures ANOVA assessed whether longitudinal accumulation of HAEs altered the average value of FA or MD, as computed for each subject over the WM skeleton at each acquired session—i.e., $\overline{\text{FA}}_{\text{WM,j,i}}$ and $\overline{\text{MD}}_{\text{WM,j,i}}$, where for $j \in \text{FBA}$: $i \in \{Pre, In1, In2, Post\}$; and for $j \in \text{NCA}$: $i \in \{Test, Retest\}$. Additionally, based on the prior assumption that DWI measures for FBA might recover toward baseline (i.e., *Pre*) once exposure to HAEs ceases at the end of the season, a repeated measures ANOVA was conducted only on the "in-season" sessions—those acquired while HAE exposure was expected to be increasing from zero (i.e., *Pre*, *In1*, and *In2*). In all relevant cases, the Shapiro-Wilk test for normality (at each session) and Bartlett test of sphericity were conducted to ensure the validity of using a repeated measures ANOVA. The non-parametric Kruskal-Wallis one-way ANOVA was used if the nor-

mality assumption was violated, and the Huynh-Feldt correction method was used if the sphericity assumption was violated. When significant differences were observed, pairwise comparison *post hoc* tests were conducted on the (subject-level) average values of FA (or MD) in the corresponding population to identify those sessions that significantly differed in mean (i.e., estimated marginal mean). Note that we consider data outside 2.5 times the interquartile range—i.e., the difference between the 75th and 25th percentiles—as outliers and excluded such data from these analyses.

Group-level regions of WM alteration: To evaluate the spatial extent of the brain in which alterations in FA or MD were observed at each session, the subset of ROI_{WM} exhibiting significant alteration in the members of the FBA group was identified as a primary region of interest for subsequent analyses—ROI_{ALT}. This group-level region was generated as follows. First those voxels were identified at each follow-up session (i.e., *In1*, *In2*, *Post*) that were significantly changed from *Pre*, as determined by a voxel-wise permutation paired t-test (50,000 permutations). Second, threshold-free cluster enhancement (TFCE) was applied on the statistics, and results were family-wise error (FWE)-corrected [91]. Finally, the subsequent union, over all follow-up sessions, of those voxels that exhibited $p_{FWE} < 0.05$, defined the group-level altered WM region, ROI_{ALT}. See Fig. 2.2 for the diagram of this process. WM tracts comprising ROI_{ALT} were identified through matching with the JHU ICBM-DTI-81 White-Matter Labels [92]. To confirm that this approach had identified a subvolume of the white matter skeleton that exhibited significant changes in mean FA and mean MD, the repeated measures ANOVA and *post hoc* pairwise comparison of sessions outlined above were repeated, but now focusing only on the voxels in ROI_{ALT}.

Subject-specific extent of WM alteration – change masks for FA and MD: Individual subject changes during and after exposure to HAEs were obtained through subject-specific quantification of extent of significantly-altered FA (or MD) values. First, for those voxels in ROI_{WM} in which the distribution of changes in FA (or MD) passed the Shapiro-Wilk test for normality, a 95% confidence interval (CI) was constructed from the NCA pool based on FA (or MD) changes observed at *Retest*
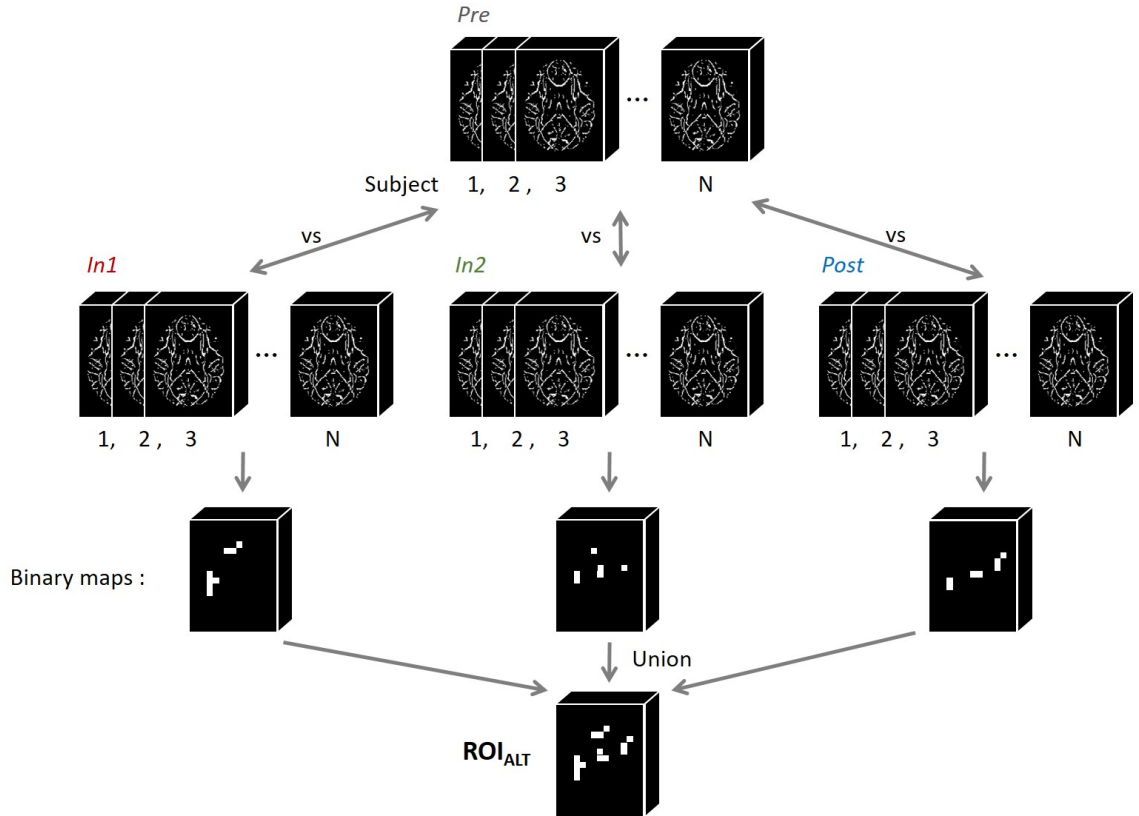
Fig. 2.2. The Diagram shows the procedures to identify the group-level extent of WM alteration in FBA relative to baseline.

relative to *Test*. Second, a "change mask" was created for each athlete (FBA and NCA) at each follow-up session (FBA: *In1*, *In2*, and *Post*; NCA: *Retest*), through identification of those voxels in ROI_{WM} for which the change in FA (or MD), relative to *Pre*, fell outside the corresponding voxel-specific NCA 95% CI. We have considered voxels for which the observed FA (or MD) change fell outside the 99.9% CI likely to be erroneous, and have excluded such voxels when creating subject-specific masks. The resulting change masks ($\text{roi\_}\Delta\text{FA}_{\text{WM,j,i}}$, $\text{roi\_}\Delta\text{MD}_{\text{WM,j,i}}$) represent subject-specific volumes of significant change for the corresponding measure. See Fig. 2.3 for the flowchart of this process.
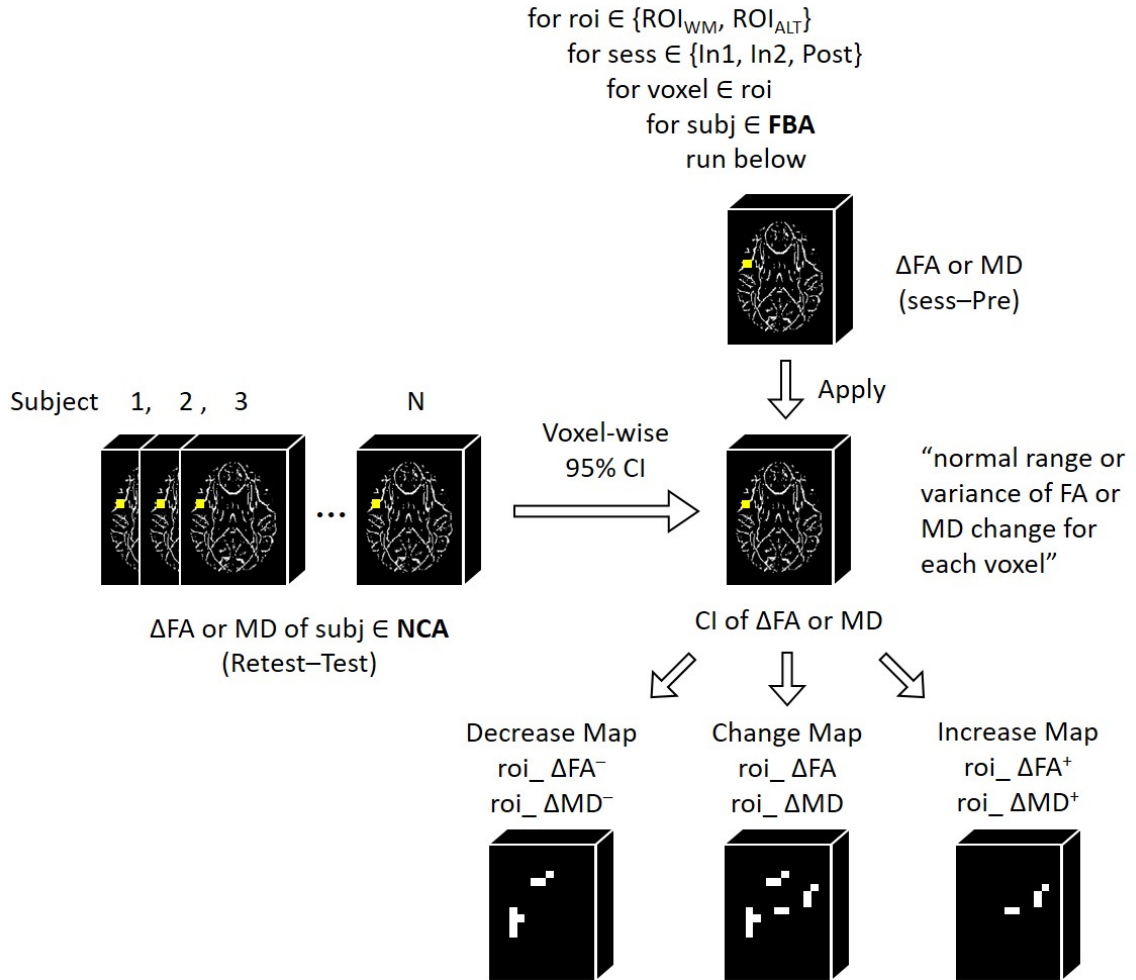
Fig. 2.3. The Diagram shows the procedures to generate the voxel-wise confidence interval map of FA and MD change and subject-specific change masks for FA and MD subsequently.

The individual-level masks generated from ROI_{WM} were intersected with ROI_{ALT}, to determine subject-specific volumes of changes in FA and MD ($\text{roi\_}\Delta\text{FA}_{\text{ALT,j,i}}$, $\text{roi\_}\Delta\text{MD}_{\text{ALT,j,i}}$) that are co-located with group-level alterations.

Subject-specific extent of WM alteration – signed change masks for FA and MD: Eight additional "signed change masks" were generated for each FBA and NCA subject, at each follow-up session, by identifying in each of ROI_{WM} and ROI_{ALT} the subset of FA or MD change mask voxels exhibiting a substantial increase

(i.e., accepted changes from *Pre* above the upper 95% CI bound; $\text{roi\_}\Delta\text{FA}^{+}_{\text{WM,j,i}}$, $\text{roi\_}\Delta\text{MD}^{+}_{\text{WM,j,i}}$, $\text{roi\_}\Delta\text{FA}^{+}_{\text{ALT,j,i}}$, $\text{roi\_}\Delta\text{MD}^{+}_{\text{ALT,j,i}}$), or decrease (i.e., accepted changes from *Pre* below the lower 95% CI bound; $\text{roi\_}\Delta\text{FA}^{-}_{\text{WM,j,i}}$, $\text{roi\_}\Delta\text{MD}^{-}_{\text{WM,j,i}}$, $\text{roi\_}\Delta\text{FA}^{-}_{\text{ALT,j,i}}$, $\text{roi\_}\Delta\text{MD}^{-}_{\text{ALT,j,i}}$). See Fig. 2.3 for the flowchart.

For each of the change masks (signed or not) created above, the percentage volumes—i.e., the ratio of the count of voxels in the change mask relative to the total voxel count in the reference mask (either ROI_{WM} or ROI_{ALT})—were compared across the FBA and NCA pools. An unpaired t-test was conducted when within-group normality was assured, and a non-parametric Wilcoxon rank-sum test used otherwise.

Regression analysis of volume of WM alteration relative to HAE exposure in FBA: For all change masks created in each of ROI_{WM} and ROI_{ALT}, linear regression analyses were conducted on the volume of change at each FBA follow-up session (*In1*, *In2*, *Post*) relative to the number of HAEs exceeding a given peak linear acceleration threshold, $Th \in \{20g, 30g, 40g, 50g, 60g, 70g\}$, experienced in practices and games up to the time of the session. For each regression, the confidence intervals for the true regression lines (i.e., confidence bands) were determined, and both Pearson (linear relationship) and Spearman (monotonic relationship) correlation analyses conducted. Regressions for which the confidence bands do not contain a slope of zero, and for which correlation achieves a significance of $p < 0.05$ are suggestive of a causal relationship between white matter alterations and exposure to repeated (sub-concussive) HAEs.

2.5   Results

HAE exposures: Table 2.2 summarizes the distribution (median, 1st and 3rd quartile) of counts of HAEs experienced by the corpus of 61 FBA in practices and games, from the beginning of the scholastic season to the time of the corresponding follow-up sessions (*In1*, *In2*, *Post*).

Table 2.2.

Distributions of "to-date" HAE exposures exceeding $20g$ as of each follow-up session for the 61 FBA subjects.

	Median	25th percentile	75th percentile
In1	69	38	108
In2	225	137	355
Post	298	160	467

Group-level longitudinal changes in mean FA and MD: The repeated measures ANOVA conducted on FBA through the "in-season" sessions (i.e., *Pre*, *In1*, and *In2*) revealed a statistically-significant effect of session both for average FA and average MD (Table 2.3). *Post hoc* pairwise analysis of the in-season sessions revealed significant changes in both mean FA and mean MD, relative to the *Pre* session, at both *In1* and *In2* (Table 2.4). No statistically-significant effect of session on average FA or MD was found for NCA or for FBA when considering all follow-up sessions (i.e., *Post* for FBA).

Table 2.3.

Repeated measures ANOVA for mean FA and MD in $\mathrm{ROI_{WM}}$ across the indicated sessions. The p-values were corrected with Huynh-Feldt's method if the sphericity assumption was violated.

Group	FA/MD	Sessions	F-statistic	p	Corrected-p
NCA	FA	All sessions	F(1, 14)=0.08	0.785	N/A
	MD	All sessions	F(1, 14)=0.23	0.642	N/A
FBA	FA	All sessions	F(3, 180)=2.44	0.066	0.070
	MD	All sessions	F(3, 179)=2.59	0.055	0.057
	FA	In-season	F(2, 120)=3.92	0.022	**0.022**
	MD	In-season	F(2, 119)=3.51	0.033	**0.033**

Table 2.4.

Post hoc pairwise *t*-test comparisons of in-season session measurements of mean FA and mean MD in ROI_{WM} for FBA (see Table 2.3). Duncan's method was used to correct for multiple comparisons.

Group	FA/MD	Pairwise comparisons	*t*-statistic	Corrected-*p*
FBA	FA	*Pre* vs. *In1*	-2.64	**0.013**
	FA	*Pre* vs. *In2*	-2.13	**0.035**
	FA	*In1* vs. *In2*	0.51	0.611
	MD	*Pre* vs. *In1*	2.11	**0.037**
	MD	*Pre* vs. *In2*	2.44	**0.021**
	MD	*In1* vs. *In2*	0.32	0.750

Distributions of individual-subject changes in mean FA and MD for FBA and NCA at each follow-up session ($\Delta\overline{\text{FA}}_{\text{WM,j,i}}$, $\Delta\overline{\text{MD}}_{\text{WM,j,i}}$) are shown in Fig. 2.4. Note that FBA consistently exhibit a higher rate of extreme changes (both increases and decreases) relative to NCA.

Group-level regions of WM alteration: The altered skeleton, ROI_{ALT}, obtained from analysis of FBA is depicted in Fig. 2.5. This group-level region represents 3.95% of the white matter skeleton (ROI_{WM}) and intersects with 14 WM tracts. Primary WM tracts involved in ROI_{ALT} are corpus callosum (body, splenium, and genu; 27% of ROI_{ALT}), superior longitudinal fasciculus (both left and right; 26%), limb of the internal capsule (left; 18%), corona radiata (left anterior, right posterior, and superior in both left and right; 18%), and cingulum (right cingulate gyrus; 9%). Additional involvement was found for left superior fronto-occipital fasciculus and right posterior thalamic radiation.
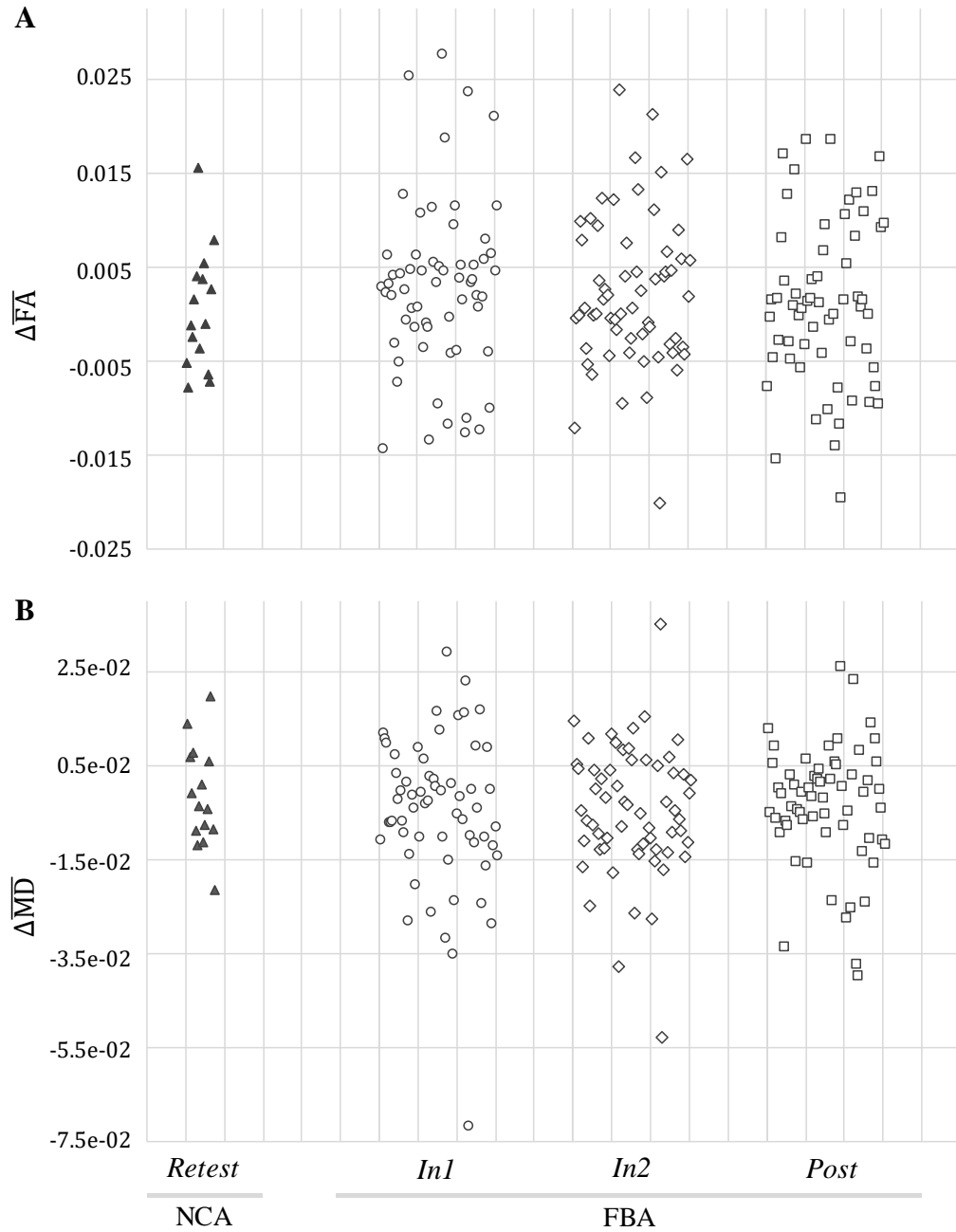
Fig. 2.4. Changes in mean FA and mean MD in ROI$_{WM}$ for FBA (N=61) and NCA (N=15) at each follow-up session compared to baseline (*Pre* for FBA; *Test* for NCA). No statistically-significant effect of session on change in mean FA or change in mean MD was found.

A

B

- Color coding
  White: WM skeleton (ROI$_{WM}$)
  Red: Altered WM region (ROI$_{ALT}$)

- Images
  A: Coronal (front) view
  B: Sagittal (left) view
  C: Axial (bottom) view

C
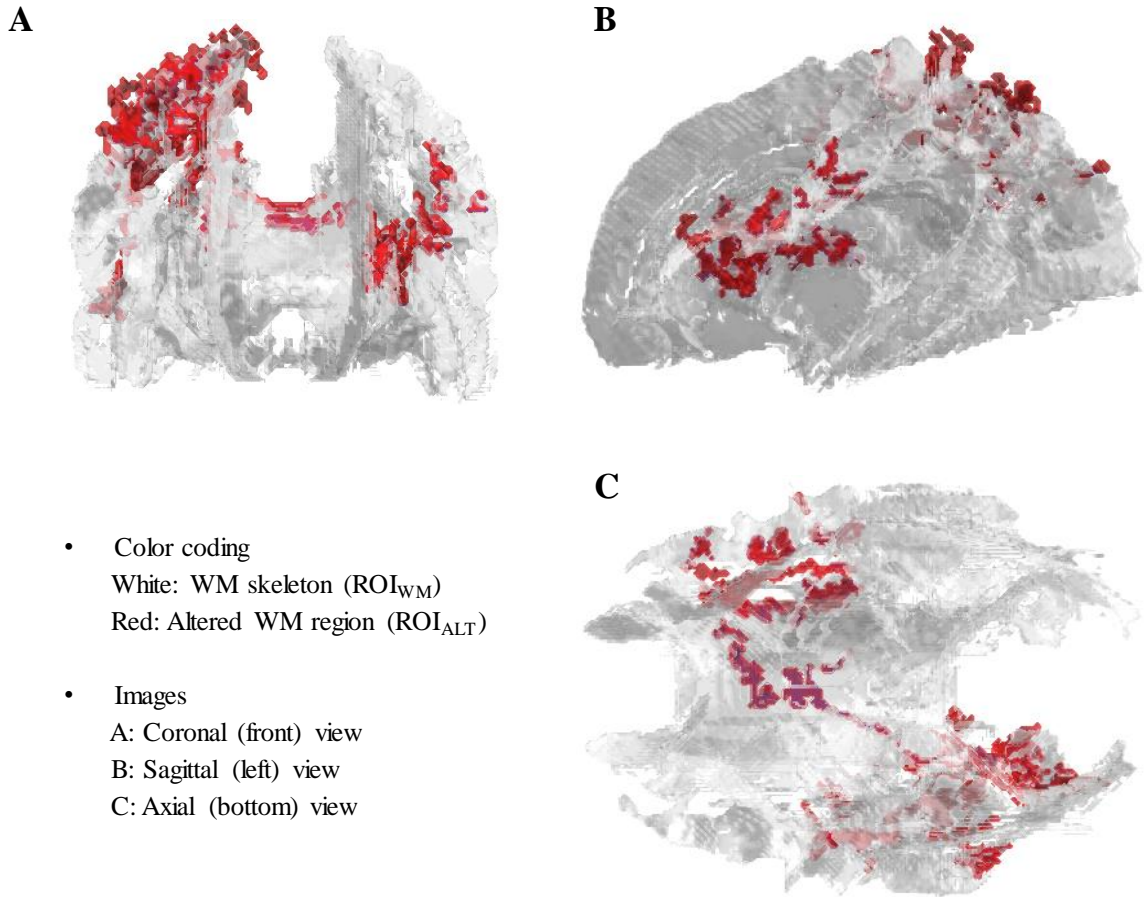
Fig. 2.5. 3D visualization (MATLAB) of ROI$_{ALT}$ depicted on a fractional anisotropy (FA) skeleton isosurface. 3.95% (comprising 14 WM tracts) of the tested volume was found to be significantly changed from the initial FA level. The detected region (ROI$_{ALT}$) was primarily found in corpus callosum (body, splenium, and genu), superior longitudinal fasciculus (left and right), limb of internal capsule (left anterior and left posterior), corona radiata (left anterior, right superior, left superior, and right posterior), and cingulum (right cingulate gyrus).

Repeated measures ANOVA and *post hoc* pairwise analysis of sessions, for both in-season analysis and analysis involving all follow-up sessions, confirmed that this volume was associated with statistically-significant changes in both mean FA and mean MD for FBA, but not NCA (see Tables 2.5 and 2.6).

Table 2.5.
Repeated measures ANOVA for mean FA and MD in ROI_{ALT} across sessions. Huynh-Feldt's method was used to correct p-values if the sphericity assumption was violated.

Group	FA/MD	Sessions	F-statistic	p	Corrected–p
NCA	FA	All sessions	F(1, 14)= 0.21	0.651	N/A
	MD	All sessions	F(1, 14)= 0.48	0.504	N/A
FBA	FA	All sessions	F(3, 180)=20.82	$< 10^{-4}$	$\mathbf{< 10^{-4}}$
	MD	All sessions	F(3, 180)= 7.91	$< 10^{-4}$	$\mathbf{< 10^{-4}}$
	FA	In-season	F(2, 120)=31.37	$< 10^{-4}$	$\mathbf{< 10^{-4}}$
	MD	In-season	F(2, 119)=10.89	$< 10^{-4}$	$\mathbf{< 10^{-4}}$

Subject-specific extent of WM alteration – change masks for FA and MD: The volumes of significant changes in FA or MD—roi_$\Delta\text{FA}_{\text{WM,j,i}}$, roi_$\Delta\text{MD}_{\text{WM,j,i}}$, roi_$\Delta\text{FA}_{\text{ALT,j,i}}$, and roi_$\Delta\text{MD}_{\text{ALT,j,i}}$—were significantly larger ($p < 0.0001$; t-test or Wilcoxon rank-sum test) at each follow-up session for FBA relative to NCA (Fig. 2.6).

Subject-specific extent of WM alteration – signed change masks for FA and MD: Consistent with the difference observed above, all signed change masks—for both ROI_{WM} and ROI_{ALT}—were found to be significantly larger ($p < 0.001$; t-test or Wilcoxon rank-sum test) at each follow-up session for FBA relative to NCA (Figs. 2.7 and 2.8).

Table 2.6.
Post hoc pairwise *t*-test comparisons of measurements of mean FA and mean MD in ROI_{ALT} for FBA using (*top*) all follow-up sessions, and (*bottom*) only in-season sessions (see Table 2.5). Duncan's method was used to correct for multiple comparisons.

Sessions	FA/MD	Pairwise comparisons	*t*-statistic	Corrected–*p*
All sessions	FA	*Pre* vs. *In1*	-7.84	**$< 10^{-4}$**
	FA	*Pre* vs. *In2*	-4.10	**$< 10^{-4}$**
	FA	*Pre* vs. *Post*	-3.19	**0.002**
	FA	*In1* vs. *In2*	3.75	**$< 10^{-3}$**
	FA	*In1* vs. *Post*	4.65	**$< 10^{-4}$**
	FA	*In2* vs. *Post*	0.90	0.367
	MD	*Pre* vs. *In1*	4.83	**$< 10^{-4}$**
	MD	*Pre* vs. *In2*	2.60	**0.014**
	MD	*Pre* vs. *Post*	1.97	0.050
	MD	*In1* vs. *In2*	-2.23	**0.027**
	MD	*In1* vs. *Post*	-2.86	**0.007**
	MD	*In2* vs. *Post*	-0.63	0.532

Sessions	FA/MD	Pairwise comparisons	*t*-statistic	Corrected–*p*
In-season	FA	*Pre* vs. *In1*	-7.92	**$< 10^{-4}$**
	FA	*Pre* vs. *In2*	-4.14	**$< 10^{-4}$**
	FA	*In1* vs. *In2*	3.78	**$< 10^{-3}$**
	MD	*Pre* vs. *In1*	4.66	**$< 10^{-4}$**
	MD	*Pre* vs. *In2*	2.51	**0.013**
	MD	*In1* vs. *In2*	-2.15	**0.033**
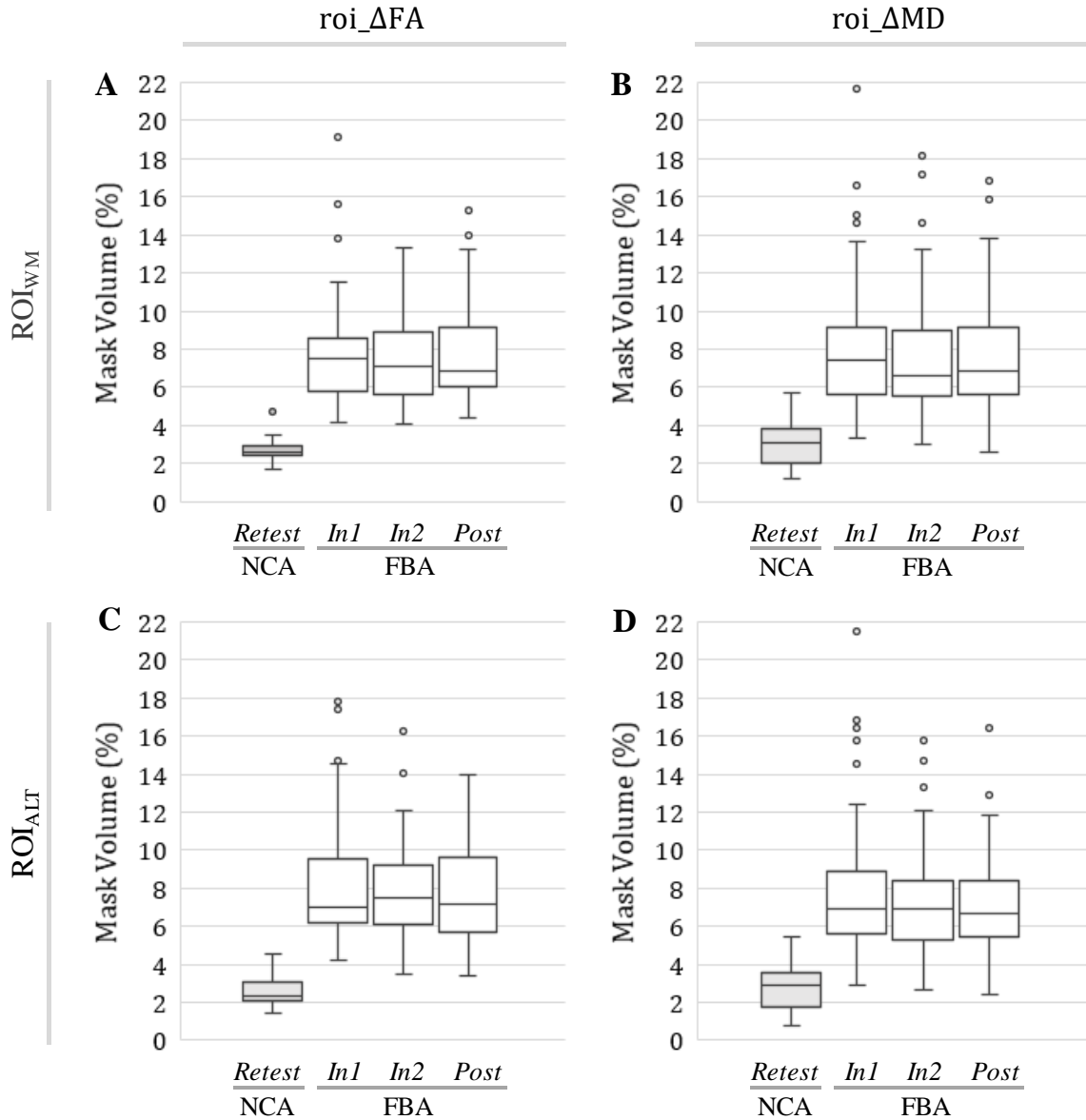
Fig. 2.6. At all follow-up sessions, football athletes (FBA) exhibited significantly ($p < 0.001$) greater volumes of significant changes in FA and MD, in both ROI_{WM} and ROI_{ALT}, than did noncollision athletes (NCA). Box-and-whisker plots are presented at each follow-up session for *(A)* $\Delta FA_{WM,j,i}$; *(B)* $\Delta MD_{WM,j,i}$; *(C)* $\Delta FA_{ALT,j,i}$; *(D)* $\Delta MD_{ALT,j,i}$.

Regression analysis of volume of WM alteration relative to HAE exposure in FBA: The most significant correlations (both Spearman and Pearson;
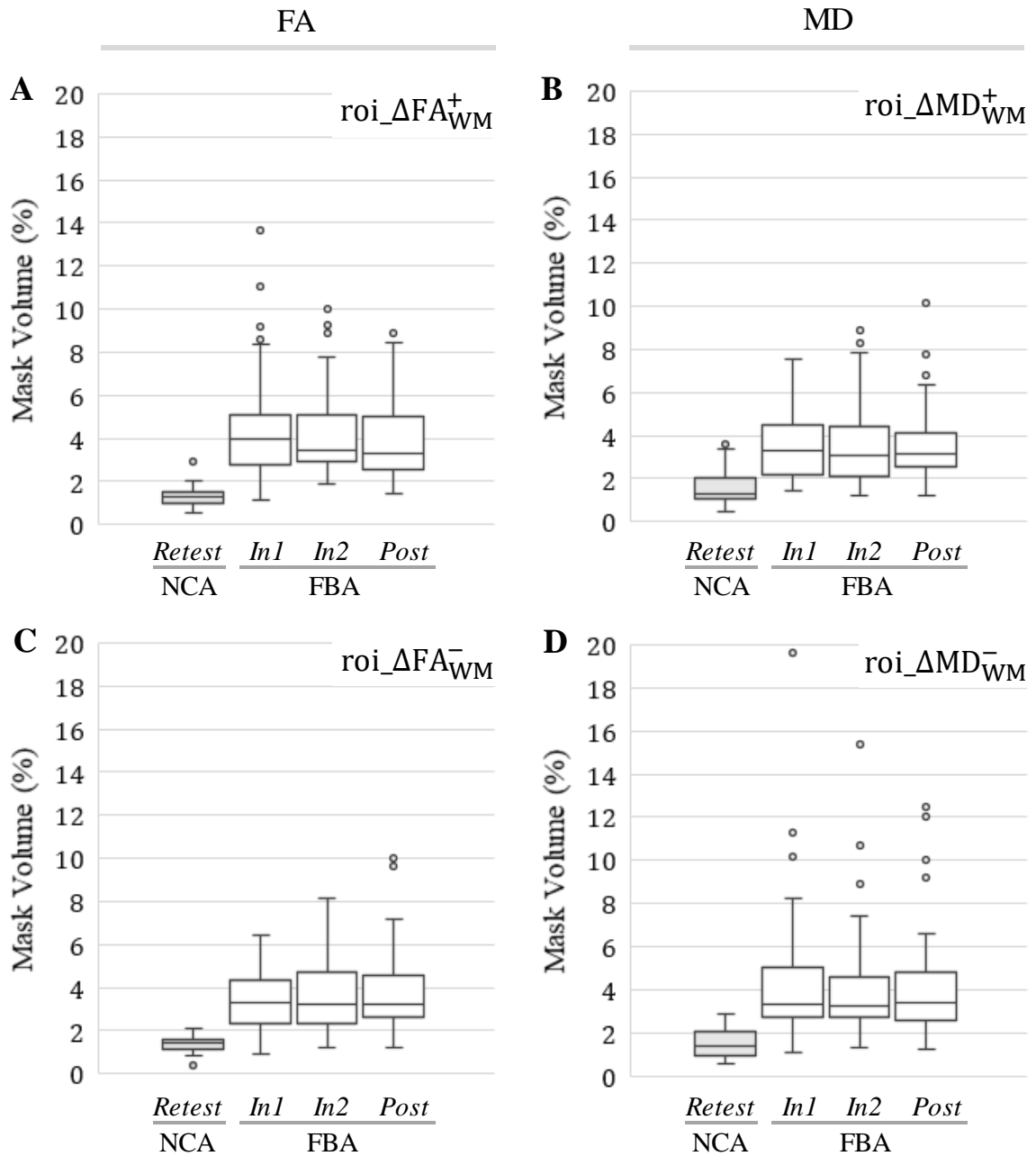
Fig. 2.7. At all follow-up sessions, football athletes (FBA) exhibited significantly ($p < 0.001$) greater volumes of significant increase/decrease in FA and MD, within ROI$_{\text{WM}}$, than did noncollision athletes (NCA). Box-and-whisker plots are presented at each follow-up session for (A) $\Delta\text{FA}^+_{\text{WM,j,i}}$; (B) $\Delta\text{MD}^+_{\text{WM,j,i}}$; (C) $\Delta\text{FA}^-_{\text{WM,j,i}}$; (D) $\Delta\text{MD}^-_{\text{WM,j,i}}$.
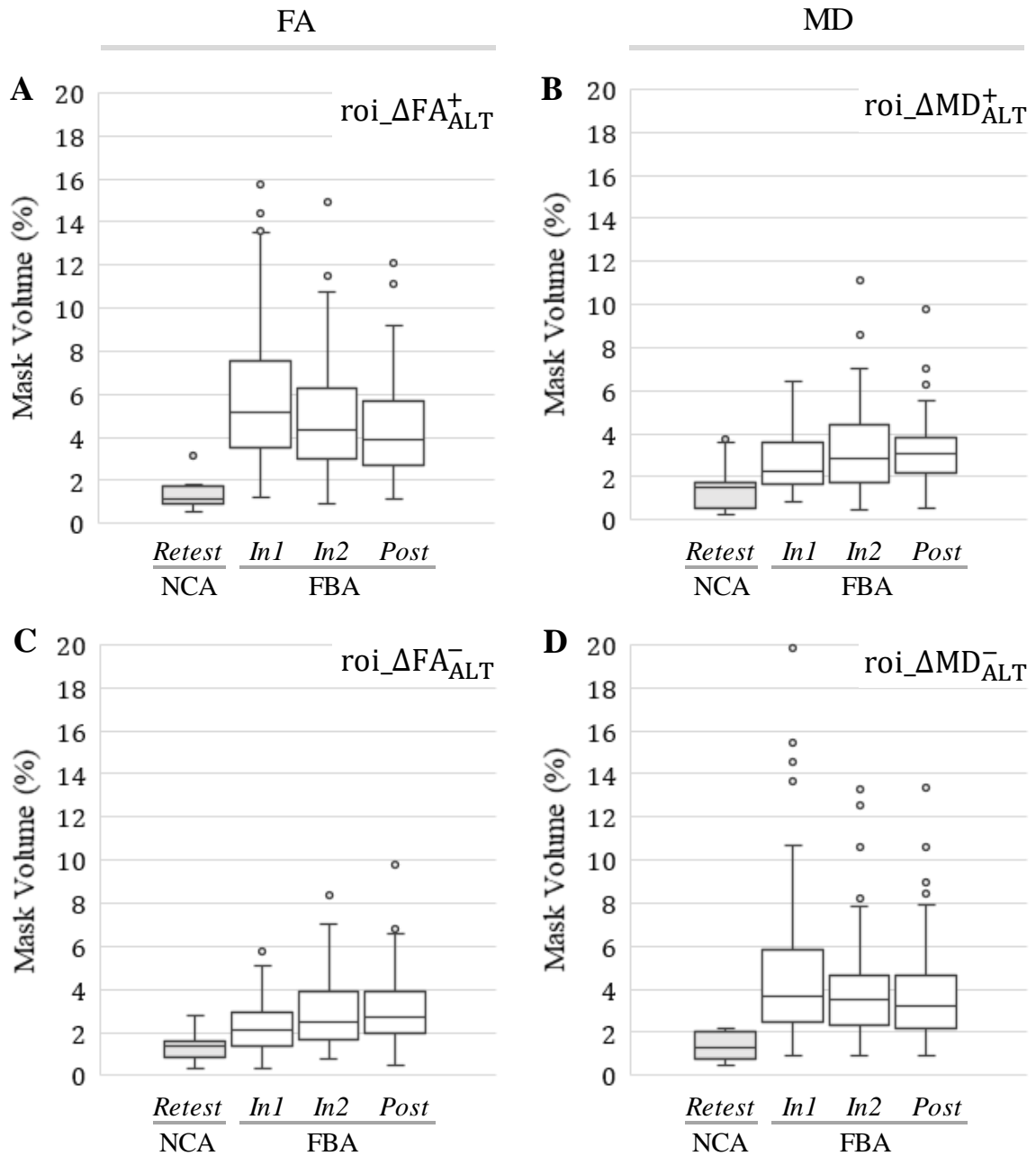
Fig. 2.8. At all follow-up sessions, football athletes (FBA) exhibited significantly ($p < 0.001$) greater volumes of significant increase/decrease in FA and MD, within ROI$_{\text{ALT}}$, than did noncollision athletes (NCA). Box-and-whisker plots are presented at each follow-up session for (A) $\Delta\text{FA}^+_{\text{ALT},j,i}$; (B) $\Delta\text{MD}^+_{\text{ALT},j,i}$; (C) $\Delta\text{FA}^-_{\text{ALT},j,i}$; (D) $\Delta\text{MD}^-_{\text{ALT},j,i}$.

see Table 2.7) were observed when comparing the to-date count of HAEs, exceeding the floor threshold of $20g$, to the signed change mask volumes for both ROI_{WM} (Fig. 2.9) and ROI_{ALT} (Fig. 2.10). For both ROIs, significant correlations with accrued HAE exposure above this best threshold were observed for increasing MD (Fig. 2.9B and 2.10B) and decreasing FA (Fig. 2.9C and 2.10C). Spearman correlation analysis also indicated a significant decrease in change volume with accrued HAE exposure for roi_$\Delta MD^{-}_{ALT,j,i}$ (Fig. 2.10D; not indicated on plot).

Table 2.7.

Pearson's and Spearman's correlation coefficients relating cumulative HAE counts exceeding the indicated linear acceleration threshold (20–70g), across all follow-up imaging sessions (i.e., *In1*, *In2*, *Post*; using the end-of-season HAE count for *Post*), to the signed change mask volumes at the corresponding times, for (*top*) ROI_{WM} and (*bottom*) ROI_{ALT}. Coefficient values achieving statistical significance are in boldface.

ROI_{WM}	$\Delta\text{FA}^{+}_{\text{WM}}$		$\Delta\text{FA}^{-}_{\text{WM}}$		$\Delta\text{MD}^{+}_{\text{WM}}$		$\Delta\text{MD}^{-}_{\text{WM}}$	
Thresh.	Pearson	Spearman	Pearson	Spearman	Pearson	Spearman	Pearson	Spearman
20g	0.0955	0.0868	**0.2361****	0.1707	**0.1698***	**0.1579***	0.0891	0.0033
30g	0.0997	0.0692	**0.2007***	0.1537	0.1303	0.1377	0.1114	-0.0147
40g	0.1253	0.0743	**0.1644***	0.1420	0.0959	0.1295	0.1429	-0.0131
50g	0.1221	0.0582	0.1221	0.1089	0.0573	0.0907	0.1268	-0.0210
60g	0.1299	0.0822	0.0846	0.0638	0.0256	0.0397	0.1214	0.0119
70g	0.1305	0.1029	0.1024	0.1132	0.0332	0.0763	0.1127	0.0175

ROI_{ALT}	$\Delta\text{FA}^{+}_{\text{ALT}}$		$\Delta\text{FA}^{-}_{\text{ALT}}$		$\Delta\text{MD}^{+}_{\text{ALT}}$		$\Delta\text{MD}^{-}_{\text{ALT}}$	
Thresh.	Pearson	Spearman	Pearson	Spearman	Pearson	Spearman	Pearson	Spearman
20g	-0.0882	-0.1021	**0.2909****	**0.2463****	**0.2605****	**0.2422****	-0.0876	**-0.1590***
30g	-0.0764	-0.1120	**0.2518****	**0.2224****	**0.2237****	**0.2267****	-0.0651	**-0.1718***
40g	-0.0487	-0.1064	**0.2044***	**0.1948***	**0.1793***	**0.2100****	-0.0332	**-0.1682***
50g	-0.0432	-0.1134	**0.1458***	**0.1531***	0.1272	**0.1710***	-0.0353	**-0.1705***
60g	-0.0210	-0.0711	0.0804	0.0833	0.2948	0.1099	-0.0196	-0.1227
70g	-0.0184	-0.0574	0.0819	0.1001	0.0727	0.1372	-0.0211	-0.1124

* Correlation significant at the $p < 0.05$ level

** Correlation significant at the $p < 0.005$ level
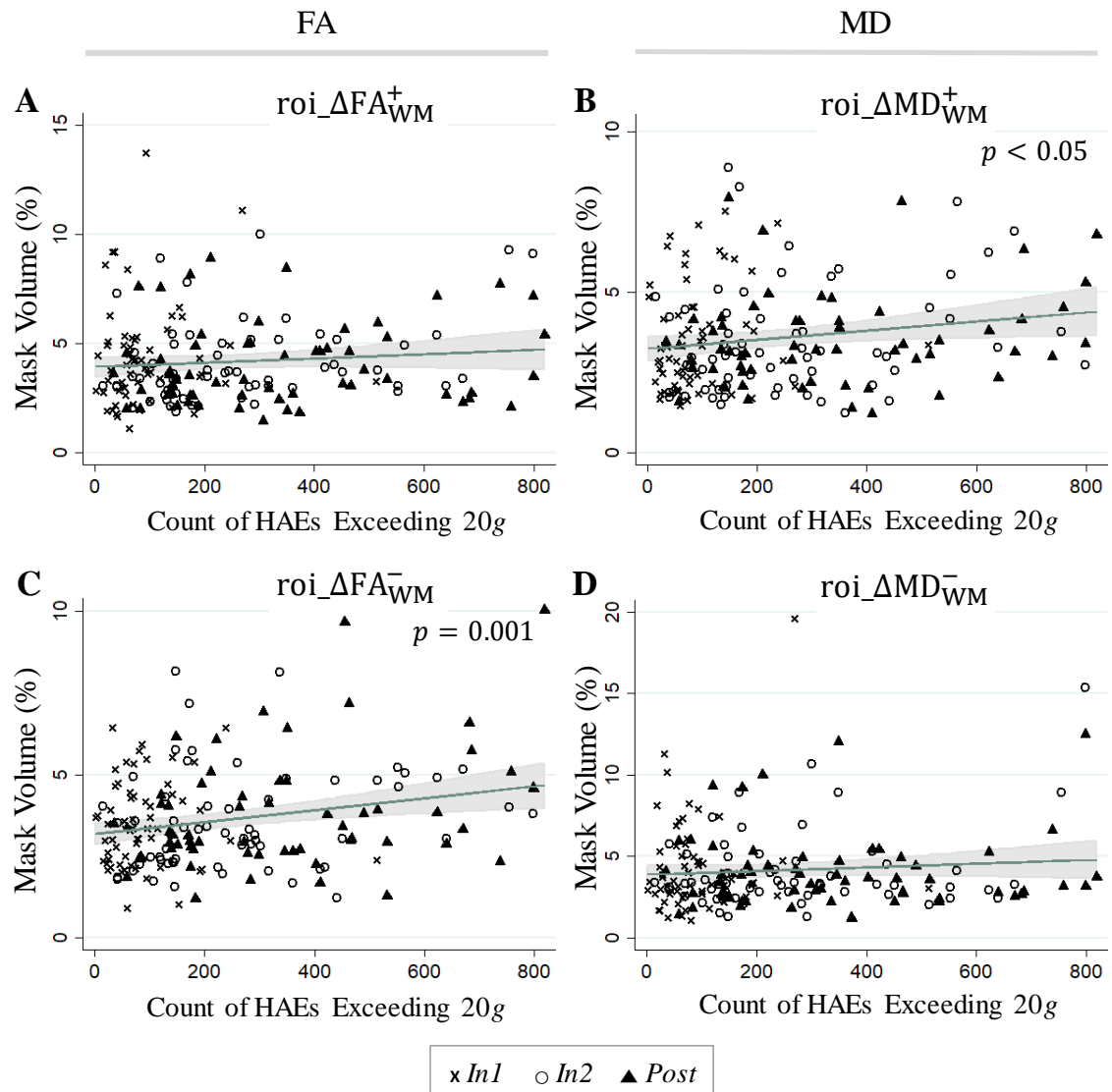
Fig. 2.9. Significant linear regressions were found for ROI_{WM} signed change volumes exhibiting significant increase/decrease in FA and MD in football athletes (FBA) as a function of the cumulative count of head acceleration events (HAEs) exceeding $20g$. Linear predictions and associated confidence bands are superimposed on 183 FBA samples (61 subjects at each of three follow-up sessions) for *(A)* $\Delta\text{FA}^+_{\text{WM}}$; *(B)* $\Delta\text{MD}^+_{\text{WM}}$; *(C)* $\Delta\text{FA}^-_{\text{WM}}$; *(D)* $\Delta\text{MD}^-_{\text{WM}}$. The white matter changes with which statistically-significant regressions were observed—increased MD and decreased FA—are typically associated with neural injury (e.g., [50, 72, 93]).
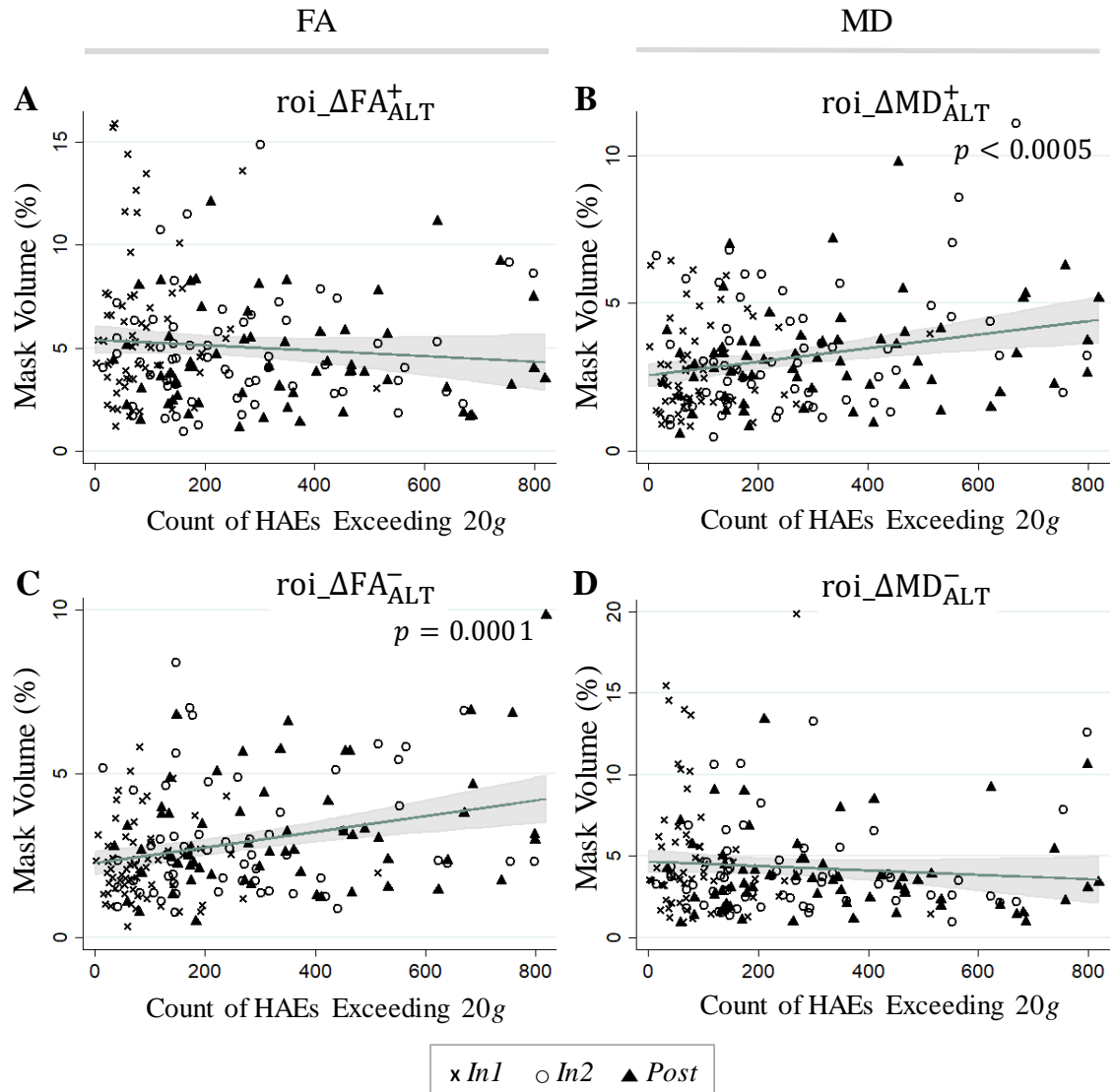
Fig. 2.10. Significant linear regressions were found for ROI_{ALT} signed change volumes exhibiting significant increase/decrease in FA and MD in football athletes (FBA) as a function of the cumulative count of head acceleration events (HAEs) exceeding $20g$. Linear predictions and associated confidence bands are superimposed on 183 FBA samples (61 subjects at each of three follow-up sessions) for *(A)* $\Delta\text{FA}^+_{\text{ALT}}$; *(B)* $\Delta\text{MD}^+_{\text{ALT}}$; *(C)* $\Delta\text{FA}^-_{\text{ALT}}$; *(D)* $\Delta\text{MD}^-_{\text{ALT}}$. The white matter changes with which statistically-significant regressions were observed—increased MD and decreased FA—are typically associated with neural injury (e.g., [50, 72, 93]).

2.6   Discussion

Retrospective examination of DWI data collected longitudinally over a single season from male high school athletes was used to test the hypothesis that athletes who experience repetitive HAEs will exhibit greater changes in white matter diffusivity than athletes who do not experience repetitive HAEs. Examination of brain volumes exhibiting changes in fractional anisotropy (FA) and mean diffusivity (MD) during and after a competition season of American football, relative to pre-participation measures, revealed appreciably greater volumes of changed FA and MD than were observed for like-aged athletes who did not experience HAEs as a core activity in their athletic competition (e.g., cross-country, golf). A novel regional analysis of signed changes in diffusion measures provided enhanced granularity of detection of pathophysiology beyond that achieved through traditional whole-brain or regional averages, and facilitated identification of volumes in which FA and/or MD either increased or decreased to lie outside the "normal" range. These change volumes developed within the first six weeks of collision activity and became larger throughout the course of the season. Critically, the extents of diffusivity changes normally associated with brain injury were found to exhibit statistically-significant correlations with cumulative HAE exposure. Such longitudinal changes, arising during, and correlated with, exposure to HAEs, support heightened public concern for athletes who participate in collision-based sports during periods of rapid brain development [94, 95]. Critically, this is the first study to document that injury-associated changes in diffusivity are correlated with accumulation of HAEs throughout the season.

FBA and NCA group-level changes in FA and MD. Statistically-significant effects were observed to exist in the whole-brain white matter mean FA and mean MD for FBA (Tables 2.3 and 2.4) only during the period of exposure to repetitive HAEs (i.e., when *Post* was omitted), suggesting that mechanically-induced neural or axonal damage is arising from this exposure. The accumulation of this damage appears to occur relatively early in the season, and subsequently asymptote—no differences

were observed between measurements acquired in the first half (*In1*) and second half (*In2*) of the season. A similar trend exists for the observed changes, relative to *Pre*, in mean FA and mean MD for FBA. Of particular interest, these mean measures exhibit larger ranges for FBA than NCA (Fig. 2.4)—consistent with the observation of [20]—but appear to arise by *In1*, and arguably stabilize, or even shrink, through the *Post* session. This apparent in-season stability may represent a steady-state balance between the accumulation of damage from continued exposure to HAEs and natural repair processes. Such an hypothesis is partly supported by the lack of an effect of session when the *Post* assessment is included, which could readily be explained by variable rates of recovery across individuals.

FBA group-level volume of changed FA and MD. The white matter structures that were observed to be the most affected by exposure to repetitive HAEs were largely central in nature. White matter regions exhibiting significant alteration in FA and/or MD (ROI_{ALT}) at the group level were predominantly (53% of the volume) located in the corpus callosum and superior longitudinal fasciculus. These locations have previously been identified as "at risk" for diffusion changes in collision-sport athletes—*corpus callosum*: [16,57,59]; *superior longitudinal fasciculus*: [57,96]. These structures represent large fiber bundles involved in integration of the cerebral hemispheres, and are frequently implicated in higher-level processes, including motor and sensory integration, memory, attention, auditory, and general cognitive functioning [97–107].

From a biomechanical perspective, these central regions would be *a priori* expected to accumulate strain from repeated head accelerations resulting from blows to the head or body. For example, both direct blows to the head and whiplash events (associated with a blow elsewhere on the body) would be anticipated to stretch/compress white matter tracts in this region. Further, blows that are directly incident on the head would be expected to generate elastic waves that will pass through the brain, with the intersection of such paths likely to be centrally located.

Additional regions in which alterations were observed in FA and/or MD included the limb of internal capsule, corona radiata, and cingulum/cingulate gyrus. The

limb of internal capsule connects the medial and anterior nuclei of the thalamus to the frontal lobes and is associated with sensory, motor, and acoustic functions [108]. The corona radiata is known as a motor pathway [109] and contains various fibers traveling to and from the cerebral cortex [108], and the cingulum/cingulate gyrus is important to brain structure connectivity and the integration of information that it receives [110, 111] as well as is associated with behavioral, emotional, and autonomic motor functions [112–114]. The other associated tracts were superior fronto-occipital fasciculus and posterior thalamic radiation. Many of the listed tracts were also reported as changed by [57] or [96].

FBA and NCA group-level changes in volume of altered FA and MD. Low-level damage to neurons/axons in the white matter tracts appears to initiate at relatively modest levels of exposure to HAEs. FBA exhibit significantly larger volumes of white matter with altered (both increased and decreased) FA and MD, relative to NCA, by the time of the first in-season monitoring session (*In1*; see Figs. 2.7 and 2.8), with these change volumes persisting in being significantly larger than in NCA through and beyond the competition season. Given that the average interval (8 weeks) between imaging sessions for the NCA was appreciably longer than the gap between *Pre* and *In1* (upper bound: 6 weeks), we may readily rule out factors such as the effects of natural maturation of white matter and changes induced by intensive exercise.

FBA regression analysis of volumetric changes with accumulated HAE count. The regression analysis conducted here strongly suggests that all athletes in collision-based activities are repeatedly experiencing low-level neural/axonal injury as a normal consequence of participation. Critically, the low-level cellular damage, observed above to arise early in the season, was found to persistently grow with continued exposure to HAEs, with a best fit achieved for the lowest acceptable HAE threshold used herein (20g; see Table 2.7). The volumes of white matter in which *(a)* FA was found to decrease over time, and *(b)* MD was found to increase over time, were both observed to exhibit a statistically-significant growth across in-season sessions. These trends are visually apparent (see Fig. 2.10) when focusing on ROI_{ALT}—those

regions of the brain that were found to differ at follow-up sessions (*In1*, *In2*, *Post*) relative to the pre-participation measurement (*Pre*)—but remained apparent even when the entirety of the white matter skeleton (ROI_{WM}; Fig. 2.10) was considered. Some additional evidence exists for decreases in MD to become more prevalent with increasing exposure to subconcussive blows, at least within the region of the white matter skeleton that exhibits significant differences at follow-up sessions (*In1*, *In2*, *Post*), relative to before participation (*Pre*). This indicates that essentially every hit matters with regard to producing damage to axons or their associated myelin sheaths.

On the nature of HAE-induced subconcussive brain injury. While none of these FBA were diagnosed as having experienced a "concussion", it would seem inappropriate to claim that these subconcussive blows have not resulted in injury. Rather, we again see support for an accumulation mechanism, whereby small amounts of damage accrue with every experienced HAE and natural repair processes are sufficient for effective recovery of these injuries until the incident HAEs include sequences of larger events for which the greater structural damage may be too much to be overcome, resulting in observation of symptoms.

It is fair to speak of damage being associated with every HAE, as the observed decreases in FA and increases in MD have been well-documented to reflect myelin damage (including demyelination) or disruption of tissue structure (including axonal damage) in the white matter. Depending on the severity of the injuries, axons may be torn, or their projections may be damaged, resulting in network disconnection. Due to the differential densities of gray and white matter, it is feasible that the incident forces will create a plane of cleavage in which axonal damage may be focused, and which would be expected to be comparably hard to repair. Note that while it is possible for microhemorrhage to occur if the small arterial branches in the gray and white matter are damaged, this outcome does not here seem likely [115].

Observation over the exposure period of increasing volumes of reduced FA and increased MD suggests that axonal and/or myelin damage is accumulating—an observation in agreement with previous reports by [72] and [11]. Critically, this ex-

pansion of the damage volume could represent the onset of less-reparable injury, as diverse forms of injury and stress-induced damage to axons (both myelinated and unmyelinated) may lead to Wallerian degeneration [116, 117].

Implications for concussion. These findings may help to clarify how concussions arise, arguing in favor of the "networking" model [48, 118] wherein focal accumulation of otherwise diffuse injury is sufficient to produce impairment in neural transmission, resulting in observable symptoms. Specifically, the diffuse accumulation of neuronal/axonal injuries may impede, but not not necessarily interrupt, the flow of information within and between any two networks. It would only be when the transfer of information through a given region of the brain (e.g., fiber tract) has become sufficiently ineffective that either the transmission or the subsequent processing are incomplete, or even precluded, leading to observable symptoms and a diagnosis of "concussion".

On the existence of a pathophysiologic injury threshold. Therefore, evidence now exists that even modest accelerations can produce *damage* to the brain tissue, but *dysfunction* is not a likely outcome until experienced accelerations exceed a notably greater, possibly accumulated, threshold (linear or rotational). This work has demonstrated that slow accumulation of changes associated with repeated exposure to HAEs that exceed $20g$ need not necessarily produce symptoms. From a circumstantial perspective, researchers have also found that retired American football athletes (who have extended histories of exposure to subconcussive impacts) may have a higher risk of developing neurodegenerative disorders such as chronic traumatic encephalopathy, Alzheimer's disease, and Parkinson's disease [7, 8, 11, 23, 24]. Conversely, it is well-documented in the traumatic brain injury literature that even single, appreciably larger acceleration events (e.g., hundreds of g) can produce readily-observable dysfunction [73, 119, 120]. Somewhere in between, then, would seem to lie the threshold at which the strains associated with an acceleration event transition from damaging the cellular membrane to rapidly, even instantaneously, affecting cellular behavior.

Our present work suggests that this pathophysiologic injury threshold is consistent with HAEs having a linear acceleration of approximately $50g$. Specifically, we have observed correlation with total exposure to events exceeding $50g$ for reductions in cerebrovascular reactivity [43], or alterations in brain chemistry, as assessed by MR spectroscopy [46].

Knowledge of a pathophysiologic injury threshold is of significant interest, as it provides a design criterion against which the development of protective and preventative measures may be assessed. Conceptually, the successful design of protective equipment, changes to rules (e.g., [121]), or improvement of athlete technique such that the number of experienced HAEs exceeding this threshold is reduced to near zero, should largely eliminate the development of symptoms within the confines of a competition season, and potentially across multiple seasons.

On the nature of changes observed in mTBI diffusion studies. These findings may also provide some insight into existing controversies on the direction of diffusivity change in white matter, caused by head trauma. Most studies that investigated severe TBI have reported that FA is decreased in major fiber tracts (e.g., corpus callosum). However, in the realm of mild TBI, observations have been more variable, with some studies observing reduced FA (and elevated MD) and some—including many sports-related studies—reporting increased FA (and decreased MD). Increased FA and decreased MD in the presence of impact-acceleration forces to the head may be explained by axonal swelling due to the injury outside the axon [19,71] or cytotoxic edema and inflammation [65, 69, 122] possibly resulting from ion homeostasis failure and membrane dysfunction [65].

Critically, the majority of studies have focused on identifying the *direction* of diffusivity change through averaging over large volumes of white matter. However, considering that the tissue encompassed by the thousands of voxels in a given region neither experience the same mechanical forces nor have the same underlying microstructure, we would expect that the severity or even nature of the injury within a given region or tract could vary. This finding is supported by our observation of mul-

tiple, sparsely-distributed locations in the white matter that exhibit either increases or decreases in FA and MD. When examined on a regional basis, these distributions generally led to changes in FA and MD that fluctuated between increases and decreases across sessions. Therefore, we hypothesize that the variation in reported results partly reflects the predominant state of injury or recovery of tissue in each region at the time of assessment.

Limitations of the present study. We must keep in mind that the exact relationship between diffusion MR markers of white matter and underlying tissue structure is still a matter of debate. Myelin and cellular membranes each play a role in restricting water diffusion in the nervous system [123–125], with cellular membranes creating boundaries between water pools of different mobility. Thus, there may not exist a strict one-to-one relationship between a given structural alteration and a particular MR measure. For example, FA may increase as a result of restricted axial diffusivity, facilitated parallel diffusivity, or some combination of the two.

Although the study incorporates an age-appropriate and gender-matched non-collision sport control population that adjusts for confounds such as environmental factors [126–128] and exercise [129], several additional extensions of the study would improve the findings. First, it would be ethically desirable to achieve a greater balance of racial and ethnic categories across the subject populations. While the FBA population was reflective of the underlying demographics of the participating schools, the acquired NCA population was skewed. This complication arose from multiple-sport participation by the underrepresented minority population at the participating schools (e.g., many track athletes also participate in football or soccer). Drawing from a broader number of schools, or schools having larger underrepresented minority populations should reduce this overlap and diversify the NCA source pool. Second, individuals in this age bracket are experiencing many biological changes, including rapid growth of the brain [130–133]. Collection of a longer-term longitudinal dataset for the NCA population, comparable to that of the FBA population, would facilitate more powerful parallel comparisons.

In a study of athletes involved in collision-based sports, it must also be acknowledged that participants may be exposed to HAEs outside the known times of practices and games, possibly through non-sanctioned play or involvement in other collision-based activities (e.g., club sports). Coupled with such additional potential exposure, complete knowledge of the use of anti-inflammatory drugs (e.g., aspirin, ibuprofen, naproxen) is unknown, and such medications could affect measurements of diffusion, particularly if the associated control of inflammation is variable across measurement sessions.

Finally, the use of traditional, single b-value diffusion weighted imaging is partially limiting, as complex white matter structures (e.g., crossing fibers) will potentially invalidate the assumption of a primary orientation of fibers, as assumed to be represented by the diffusion tensor's main eigenvector [134]. A longitudinal approach that applies a more powerful technique such as diffusion kurtosis imaging could provide additional insight.

2.7 Conclusion

This is the first study to document that changes in diffusivity of white matter associated with neuronal injury are correlated with accumulation of head acceleration events throughout the course of a season of participation in a collision-based sport. High school-aged athletes participating in American football were found, in all sessions acquired during and after their competition seasons, to have greater volumes of white matter exhibiting decreases in fractional anisotropy (and increases in mean diffusivity) than their peers who compete in non-collision-based varsity sports. Combined with prior work studying when abnormal physiologic responses arise, this work strongly suggests that every experienced head acceleration event causes some level of injury, with the accumulation of larger head acceleration events being necessary for natural repair processes to be overwhelmed. Future effort should be directed at reducing the number and magnitude of events experienced by collision-sport athletes,

whether through enhanced protective equipment, improved technique instruction, or modification of rules.

2.8   Acknowledgments

3. CONVOLUTIONAL NEURAL NETWORK-BASED QUALITY CONTROL OF DIFFUSION TENSOR IMAGING THAT DOES NOT REQUIRE A BIG DATASET

3.1 Abstract

Diffusion tensor imaging (DTI) is a versatile imaging modality, which allows precise and non-invasive assessment of the microstructure in white matter. However, the complex nature and long acquisition time associated with DTI make it susceptible to artifacts that may result in inferior diagnostic image quality. Despite many efforts to detect and correct artifacts, there is still a need for experts to identify corrupted images through visual inspection. We present an automated quality control (QC) pipeline that uses transfer learning of a deep convolutional neural network. The QC pipeline detects not only motion- or gradient-related artifacts but also many kinds of abnormal acquisitions, such as images with regional signal loss or that were incorrectly imaged or reconstructed. The greatest benefit of the proposed QC method is that it provides high detection accuracy without the need for a large dataset to train the model. Other advantages include a high speed of image testing, an ability to detect various artifacts, and the potential to be generalized across multiple sites.

3.2 Keywords

Image Quality Assessment, Diffusion Tensor Imaging, Convolutional Neural Network, Transfer Learning, Quality Control

3.3 Introduction

Diffusion Tensor Imaging (DTI), which is acquired by processing diffusion-weighted imaging (DWI) data, is a well-established and powerful imaging technique that can non-invasively probe the integrity and orientation of white matter fibers in the brain [26, 27]. However, one major challenge of DTI studies is the acquisition of high-quality images. Due to inherent limitations of acquisition, DTI suffers from inter-slice and/or intra-slice intensity artifacts typically due to interaction between a subjects motion (e.g., body movement, cardiac pulsation) and diffusion encoding as well as from checkerboard artifact, ghosting artifact, and susceptibility effects [27]. DTI also suffers from a regional signal loss, erroneous imaging or reconstruction, and a relatively low signal-to-noise ratio (SNR), which hinders accurate estimation of DTI parameters, interpretation, and reproducibility [28, 29]. Images containing one or more of these artifacts need to be identified and either considered for further processing or excluded from the analysis. This identification procedure that is used to ensure that only quality data are included in subsequent analyses is called quality control (QC) or quality assessment (QA); these two terms are used interchangeably in this work.

The current QC gold standard involves a visual and manual inspection of the data. However, visual inspection is quite difficult and time-consuming, especially for DTI in which many volumes are acquired for each subject. Given the number of correction stages in a typical DTI processing pipeline, and the large number of slices associated with an acquisition, it is desirable to have an automated and quantitative QA process. Quantitative QC approaches have been established that focus on identifying and reducing specific artifacts, including geometric distortion artifacts induced by the combination of eddy currents [30] and motion [28,31], and general noise reduction [29]. These efforts have been applied to both acquisition and post-processing stages [28] and relevant tools are publicly available [31–34, 135]. Although promising, these approaches still require significant effort on the part of investigators, are capable of

detecting only a specific type of artifact, or report lower performance than visual inspection. For these reasons, the primary method of QC in many hospitals and research groups still consists of a manual and visual inspection.

One approach for developing an automated QC process for a large number of images would be to use a supervised learning approach based on machine learning [35,36] or deep learning algorithms, such as a convolutional neural network (CNN) [37]. The CNN is a class of neural network, which has been successfully used in various computer vision problems such as object detection, image segmentation, and video classification as well as in identifying motion artifacts in structural [136] and diffusion MRI [137, 138]. Different from other learning approaches, CNNs learn features from the data (typically image) during training, rather than requiring features to be hand-crafted and supplied by a human. A CNN containing many layers is referred to as a deep CNN (DCNN). While offering high classification accuracy, DCNNs can be time-consuming and are expensive to train (possibly several weeks or days, even with a high-performance GPU). The *Transfer Learning* [38] technique is often used to reduce learning time and to achieve better performance and is particularly useful when the size of a dataset is small relative to the complexity of a model to be trained. Transfer learning uses weights from a network that was trained for a different, but related, domain or task.

This work presents an algorithm based on a DCNN transferred from a heterogeneous domain, which enables fully automated QA of DTI. DTI data from only 90 subjects are needed to train the neural network. Considering that there is a relatively small dataset, that computational resources are limited, and to take advantages of a 2-D DCNN that was well-designed and trained, 2D slice images were extracted from each DTI volume that were then labeled (whether they contain an artifact or not) by two analysts. We decided to reject a DTI volume if it has more than two slices exhibiting an artifact. Data augmentation was performed by shifting and flipping the images and the augmented data was supplied as input to the DCNN. We evaluated the

performance of this DCNN and provided a receiver-operating characteristic (ROC) that can enable users to determine a task-specific threshold to optimize performance.

3.4 Methods

3.4.1 Data Collection

Data previously collected from 90 adolescents (age 14-18 years; average $= 16.6$ years) were evaluated in this study. The cohort was comprised of both males and females who participated in a variety of sports. Each subject underwent one MRI session on a 3T General Electric Signa HDx using a 16-channel brain array. Diffusion weighted images were acquired using a two-dimensional single-shot spin-echo echo-planar imaging sequence with the following imaging parameters: repetition time (TR)$=12000ms$, echo time (TE)$=83.6ms$, flip angle$=90$ degrees, field of view (FOV)$=240mm \times 240mm$, spatial resolution$=2.5mm \times 2.5mm$, slice thickness$=2.5mm$, slice gap$=0mm$, 46 contiguous axial slices, frequency readout$=$R/L. 30 diffusion-weighted directions were acquired with $b=1000$ s/mm^2, and one volume acquired with $b=0$ s/mm^2. Raw images were reconstructed by the GE machine with $0.938 \times 0.938 \times 2.5mm^3$ resolution for each direction, yielding $256 \times 256 \times 46 \times 31$ voxels for each scan.

3.4.2 DTI Image Processing

Raw DICOM images were converted to the NIfTI format using *dcm2nii* [139] and b-vectors and b-values were extracted from the DICOM headers. FSL 5.0 [78,79] was primarily used for processing the images. Brain segmentation was performed based on the non-diffusion-weighted (b=0s/mm^2) volume. By fitting the diffusion tensor

model at each voxel, scalar diffusion tensor maps, including three eigenvalues, were obtained. Fractional anisotropy (FA) was computed by:

$$FA = \sqrt{\frac{3}{2}} \cdot \sqrt{\frac{(\lambda_1 - \bar{\lambda})^2 + (\lambda_2 - \bar{\lambda})^2 + (\lambda_3 - \bar{\lambda})^2}{\lambda_1^2 + \lambda_2^2 + \lambda_3^2}}$$

where $\bar{\lambda} = (\lambda_1 + \lambda_2 + \lambda_3)/3$ and each eigenvalue represents the length of an axis in the tensor; i.e., the displacement or diffusion along each corresponding eigenvector. The resultant FA volume has $256 \times 256 \times 46$ voxels for each scan.

3.4.3   Ground Truth Annotation

Supervised learning was adapted where data needed to be labeled to form input-output pairs for training. All scans were visually inspected by two trained analysts. Images that appeared to contain artifact(s) were recorded. Such artifacts included striping caused by motion, defective gradient performance, inter-slice or intra-slice signal dropouts, severe signal loss, metallic object-induced artifacts, and checkerboard artifacts. The number of images in each volume with artifact(s) was recorded. A 3–D volume was considered "poor" if more than two slices contained an artifact or "good" otherwise. Volumes for which labeling did not match between the two analysts were not used in the study.

3.4.4   Dataset Configuration

Given that FA is considered to be a summary measurement of microstructural integrity and is sensitive to changes therein, FA volumes were used for QA. In the NIfTI format, an FA has 16-bit channels with intensity ranging from 0 to 1. Rather than directly using 3–D FA volumes for QC, we decided to supply the QC model with multiple 2–D slice images for the following reasons: 1) to increase the number of elements available for training the DCNN and 2) due to limited availability of computational resources. Forty 2–D sagittal slices from around the center were extracted from each volume. It is important to collect 2–D slices perpendicular to

the imaging direction. Considering that the imaging volumes were prescribed in the axial orientation, either sagittal or coronal slices are desired for extraction because it is relatively easier to find artifacts from them. Example 2–D slices of an FA volume with artifacts can be seen in three different orientations in Fig. 3.1.
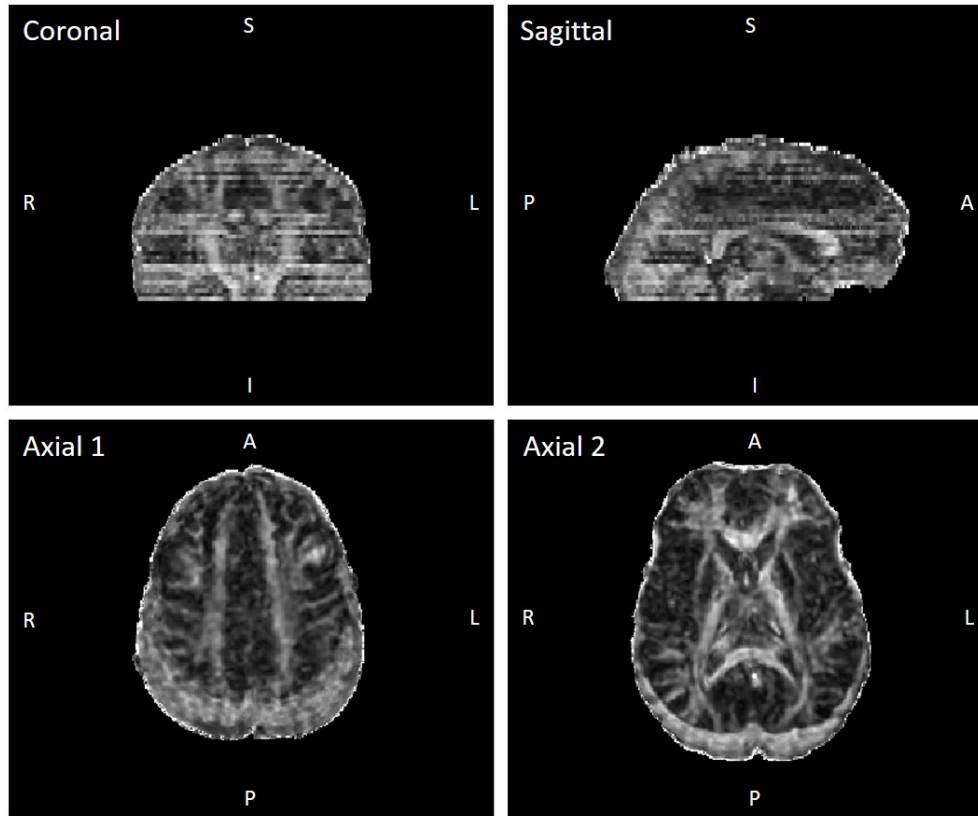
Fig. 3.1. Images of an FA volume with artifacts that can be seen in three different orientations. Artifacts can be more easily found in the sagittal or coronal slices as compared to the axial slices.

The images were zero-padded along the shorter dimension to make them square, resulting in 256×256 pixels for each image. For training pre-trained DCNNs, these 2–D slices were replicated three times to form three-channel images, which is required by the pre-trained DCNNs used in the study.

Data augmentation was performed on each 2–D slice via translations and flips. A total of 21,600 images were used to train, validate, and test QC models.

A total of 16,800 images corresponding to seventy volumes were used for training; 2,400 images corresponding to ten volumes for validation; and the other 2,400 images corresponding to ten volumes were used for testing QC models. Here, the train-validation-test split was conducted based on volume (or subject) rather than image; i.e., if an image from a volume was used for training, images from that volume were not used for validation or testing.

3.4.5 Convolutional Neural Network-Based QC

Models used in the study: Four modern DCNNs with different architectures—ResNet50, VGG19, Inception-v3, and Inception-ResNet-v2–were considered for supervised learning to perform QC on DTI. These networks have achieved state-of-the-art performance in the classification of more than 1-million natural images taken with standard cameras (e.g., flamingos, dogs, airplanes, cars) into 1,000 classes [140]. The classification of the ImageNet dataset is now a standard task in computer vision. More conventional algorithms—i.e., random forest and support vector machine—were also considered for comparison.

Transfer Learning Procedures: In order to prevent overfitting of the training data, the DCNNs that were pre-trained with the ImageNet dataset were used and retrained using the transfer learning technique, rather than training the neural networks from a random initialization. In this way, the pre-trained DCNNs were used as a baseline image feature extractor. The current work performed more subtle fine-tuning of the networks as compared to a typical transfer learning approach where only a few top layers are re-trained. In this study, the top layers of the networks, which do not involve convolution, were removed and replaced by a few layers—i.e., average pooling, dropout, fully-connected, fully-connected, and sigmoid (Fig. 3.2)—to account for the transferred task. The dropout regularization was used to reduce overfitting and the sigmoid activation function to perform binary classification. The neural networks were re-trained with the DTI data while freezing the weights on the

original layers, which is called "retraining-top-layers". This step trains only the top layers, which were randomly initialized. Then, fine-tuning of a wider range of upper layers was performed, where the first K layers were frozen and the rest were unfrozen, which is called "fine-tuning". The learning procedures are illustrated in Fig. 3.2 using the layout of Inception-v3.

Hyperparameters for Training: K is an important hyperparameter for optimization because fine-tuning of too many layers may cause overfitting. We used a dropout rate of 0.4 and 1,024 neurons for the fully connected layer and training and validation was done with a shuffled mini-batch size of 64. Training was performed to minimize the cross entropy between the estimated class probabilities and the true distribution. A stochastic gradient descent with the adaptive learning rate method (Adadelta) was used, which dynamically adapts the learning rate over time based on a moving window of gradient updates and requires minimal computation over gradient descent [141]. The maximum number of epochs for retraining-top-layers and the fine-tuning were both set to 30. Validation loss was monitored at each batch and training was stopped when the lowest validation loss for an epoch did not improve for five epochs.

The support vector machine classifier used a 4th order polynomial kernel with a coefficient (i.e., gamma) calculated as $1/(256 \times 256\times$ variance of pixel intensities), the maximum number of iterations of 400 and tolerance for stopping criterion of 0.005, kernel cache size of 5 GB, and a penalty parameter of the error term (i.e., C), which set the amount of regularization, of 1.0. The random forest classifier used 11 trees with a maximum depth of 3 for each tree, the maximum number of features to consider when looking at each split of 256, the minimum number of samples required to split an internal node of 2, and bootstrap samples were used to build trees.
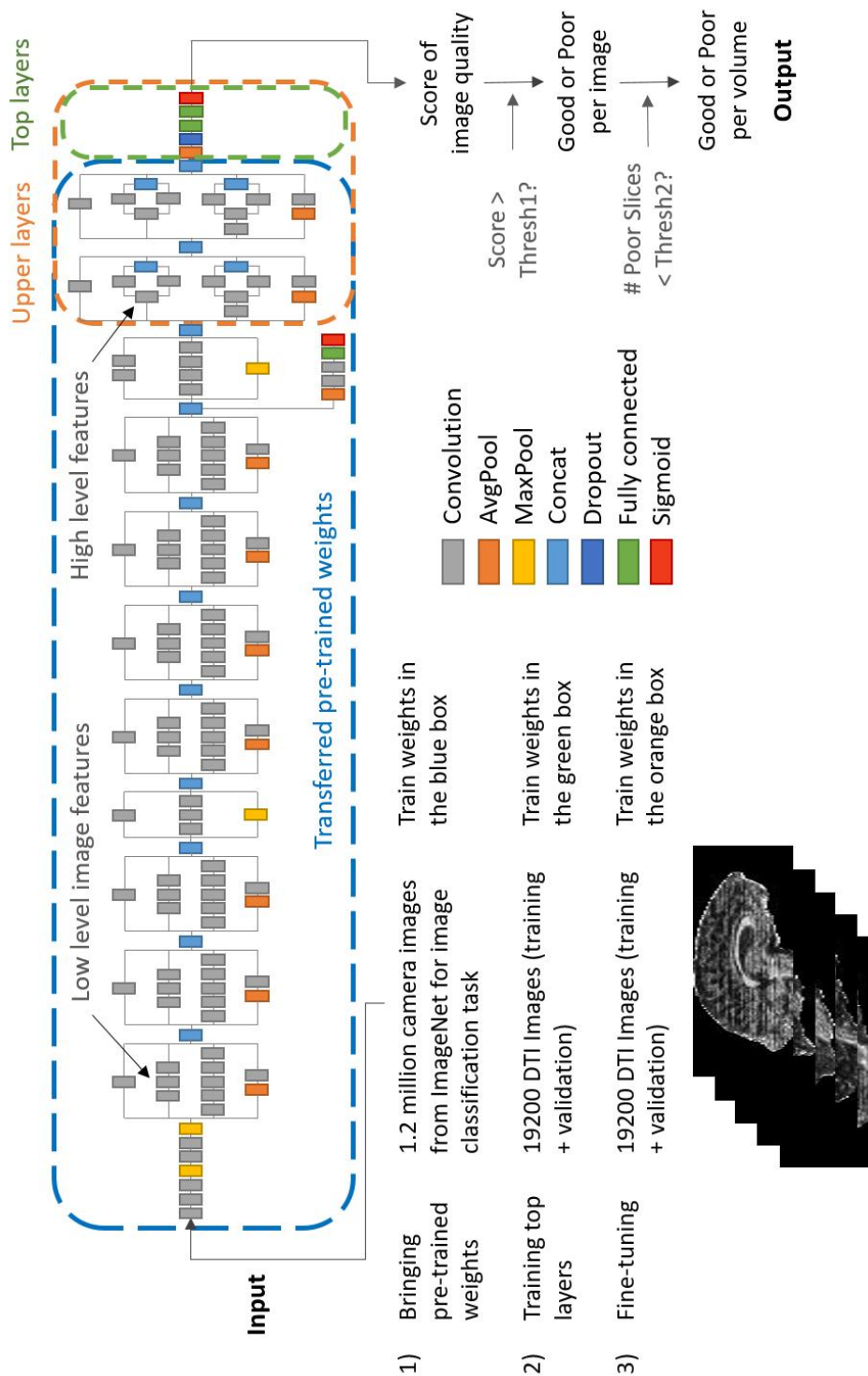
Fig. 3.2. The transfer learning procedures of DCNNs that are illustrated using the layout of Inception-v3.

3.4.6   Computational Resources and Software Frameworks

For training the neural networks, a workstation equipped with one NVIDIA Titan Xp and two Intel Xeon E5-2680 were used. The implementations were conducted using Keras-v2 [142] and TensorFlow-v1.12 distributed machine learning system [143] frameworks with CUDA-v9.0 [144] and cuDNN-v7.1 [145] as back-end. Scikit-learn-v0.20 machine learning library [146] was used for implementing the random forest and support vector machine classifiers.

3.4.7   Analysis

Validation loss and accuracy were monitored after training each batch. At the end of training, the model weights from the epoch with the lowest validation loss were restored and used for testing. The resulting fine-tuned DCNNs were then tested on the holdout test set to evaluate performance. A receiver-operating characteristics (ROC) analysis was performed and the area under the ROC curve (ROC AUC) and accuracy were computed for all six models.

3.5   Results

ROC curves at the image level classification are shown in Fig. 3.3 using the holdout test set for each of the four DCNN-based classifiers (i.e., ResNet50, VGG19, Inceptionv3, Inception-ResNet-v2), random forest, and support vector machine classifiers by shifting the decision threshold for the "poor" classification at the image level.

The summarized classification results of the four DCNNs, random forest, and support vector machine models at the image level are presented in Table 3.1, including the area under the ROC curves and accuracy. The AUC was the highest in the Inception-ResNet-v2-based classifier (99.98%), followed by the Inception-v3 and VGG-19. Accuracy was highest in the Inception-v3-based classifier (99.10%), followed
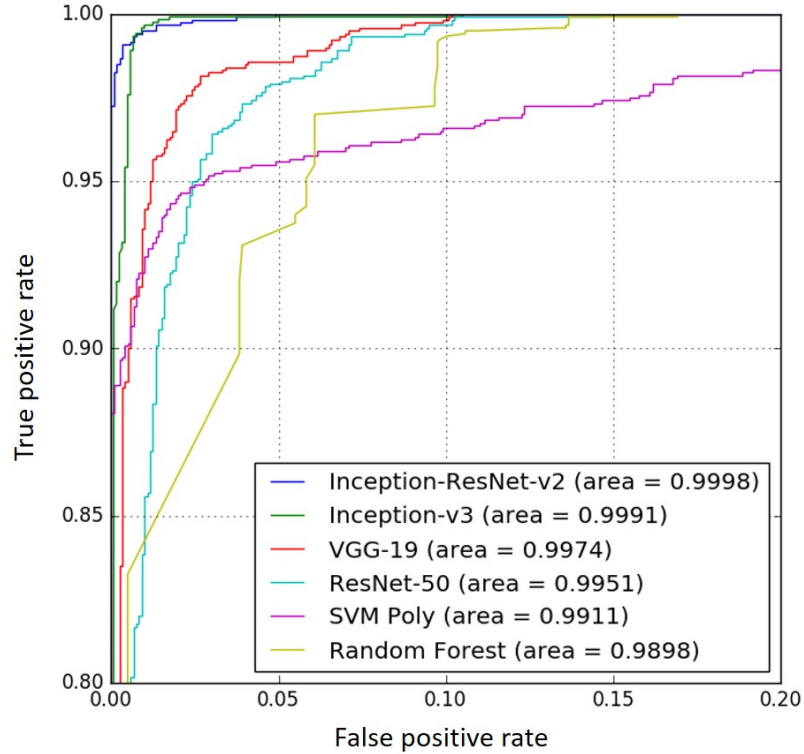
Fig. 3.3. ROC curves for the detection achieved by the six classifiers are shown. Note that true positive refers to classifying a "good" DTI image as "good".

by the Inception-ResNet-v2 and VGG-19. The last column of the table shows the relative model complexity by rank based on the total number of parameters, which can be a useful factor when two or more models exhibit similar performance. All tested volumes were classified correctly.

Selected major hyperparameters for the two highest performing models are described in this paragraph. The Inception-v3-based model has 314 layers including all activation layers. The best validation results were achieved when fine-tuning was applied to the layers above the 196th. The layers below the 632nd were frozen when fine-tuning the Inception-ResNet-v2based model, which has 783 layers. With the early stopping applied for training, none of the DCNN models exceeded 18 epochs for the retraining-top-layers and none exceeded 13 epochs for the fine-tuning. The

Table 3.1.

Classification performance of the four fine-tuned DCNNs, random forest, and support vector machine models are presented. ROC AUC and accuracy of the detection achieved by each model are provided.

	AUC [%]	Accuracy [%]	Model Complexity [rank]
Random Forest	98.98	95.46	**6**
Support Vector Machine	99.11	96.29	5
ResNet-50	99.51	96.71	3
VGG-19	99.74	97.00	1
Inception-v3	99.91	**99.10**	4
Inception-ResNet-v2	**99.98**	99.08	2

Inception-v3-based model was trained for 10 epochs for the retraining-top-layers and 7 epochs for the fine-tuning. The Inception-ResNet-v2-based model was trained for 10 epochs for the retraining-top-layers and 5 epochs for the fine-tuning. Training required approximately 30 minutes for both models on a workstation equipped with a Titan Xp. Less than 40 ms were required to test each DTI image.

Both of the DCNN-based classifiers successfully detected different poor images that have one or more of the following artifacts: inter-slice and/or intra-slice intensity artifacts (typically due to interaction between subject motion and diffusion encoding), severe regional signal loss (e.g., due to braces), erroneous imaging or reconstruction parameters, checkerboard artifacts, high noise level, and ghosting artifact. See Fig. 3.4 for examples.
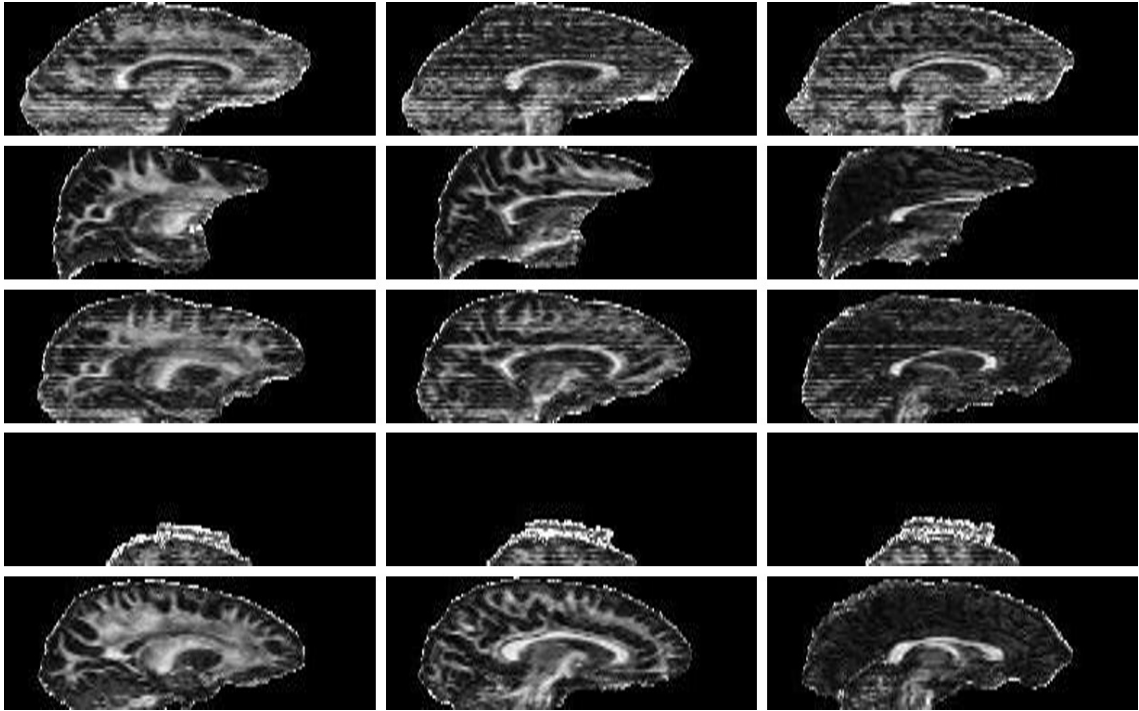
Fig. 3.4. Example of poor DTI images detected with the DCNN-based classifiers. There were images with striping, severe signal loss, inter-slice and intra-slice signal dropout, erroneous imaging or reconstruction.

3.6 Discussion and Conclusion

A pre-trained DCNN was used as a baseline feature extractor and retraining of top layers and fine-tuning of upper layers (Fig. 3.2) was performed with a DTI dataset. Predictions were made based on a subset of sagittal slices extracted from 3–D volumes. There were two rationales for this approach. First, we wanted to increase the amount of data (or element) for training by converting a 3–D volume to forty 2–D slices. Second, computational resources, particularly GPU memory size, were limited for processing 3–D volumes in very deep neural networks comprising tens (or hundreds) of millions of parameters. It is critical to collect 2–D slices that are perpendicular to the imaging direction. If the imaging volumes were prescribed in the

axial orientation, either sagittal or coronal slices are desired for extraction because image features associated with artifacts are more easily learned from them.

All four of the DCNNs (i.e., ResNet50, VGG19, Inception-v3, Inception-ResNet-v2), random forest, and support vector machine classifiers achieved an accuracy of 95% or greater. The highest performance (99% accuracy and 99.9% AUC) was achieved by the Inception-ResNet-v2- and Inception-v3-based models. These QC models were able to detect not only images with motion or gradient-related artifacts but also images with regional signal loss and erroneous imaging such as scans that were terminated before the end. Beyond high performance and the ability to detect various types of artifacts, the strength of the proposed method lies in its short inference time (less than 40 ms to test a 2–D DTI slice), reasonable duration of training time (average of 30 minutes to train the entire model with 16,800 slices and to validate with 2,400 slices), the ability to adjust the decision threshold for the "poor" classification, and the ability to be customized and generalized. The current algorithm can be further generalized by collecting images from multiple sites with a range of imaging parameters. On the other hand, the proposed method would be more powerful as a site-specific QC tool, which can be done by fine-tuning the model with data from a specific site.

The current study had several advantageous terms for classification. First, all DTI images were collected with a single scanner using the same parameters. Second, volumes in which their labeling did not match between the two analysts were not used in the study, which may have excluded volumes of moderate quality that are often hard to classify.

Even if the proposed method achieved high performance, this is not yet a generalizable score because of the small size of the test set. More data need to be collected and tested to perform additional analyses in order to prove reproducibility.

Future work will explore augmentation of the training set with more images; a more diverse pool of corrupted images would be desired. Focusing on the synthetic augmentation of images with rare artifacts would be helpful and the use of generative

adversarial networks may be considered. Furthermore, extensive efforts will be made to establish a gold standard for "good" images with different radiologists who have expertise in diffusion MRI.

4. FUTURE DIRECTIONS

4.1   Neurotrauma Study Using Diffusion Tensor Imaging

DTI has several advantages over conventional MRI and other neuroimaging tech-
niques. Because of the ability of DTI to measure spatial organization of brain tissue
with high sensitivity, it has been used to identify brain biomarkers of various neu-
rodevelopmental and neurodegenerative disorders. In the near future, extensive effort
will be placed on tracking youth football athletes for a longer term to verify the con-
clusions made in this study as well as to track non-collision sport athletes for multiple
years.

Significantly altered white matter regions were found in the football athletes at
both the group level and individual level in this work. The next step will be to verify
if the detected structural changes in white matter tracts are involved with functional
and/or biochemical alterations. A multi-modal MRI analysis will be performed that
integrates data from resting state functional MRI, which measures changes in func-
tional organization and regional interactions, and magnetic resonance spectroscopy,
which quantifies biochemical (i.e., neurometabolites) changes, that have been col-
lected for the same cohort with DTI data. Moreover, outcomes of previously col-
lected neurocognitive testing could be used to find connections between functional
connectivity in gray matter and cognitive functions.

PNG began collecting MRI data using a newer MRI machine, which is more re-
liable than previous hardware [147]. Data collected in the newer machine could be
merged with the current datasets to facilitate a long-term study involving multiple
football seasons and to achieve a larger sample size. The inter-site analyses performed
by Jang and colleagues reported outcomes that support multisite diffusion-based stud-
ies, pending confirmation of stable distributions of diffusion measurements. Future

work will validate whether measurements from the two sites can be used interchange-ably and a scaling algorithm will be developed if needed.

Although not included in this document, I have put effort into investigating longer-term effects of head impact exposure in football athletes [148] as well as identifying predictors of integrity changes in white matter [149]. The results indicated that age and ethnicity as well as history of concussion were strong predictors of persistent changes in white matter. Such findings would be reflected in the design of statistical models in future studies.

4.2   Automated Quality Control of Diffusion Tensor Imaging

An automated QC algorithm by transfer learning a deep convolutional neural network was proposed. A pre-trained DCNN was used as a baseline feature extractor and retraining of top layers and fine-tuning of wider range of layers were performed with a DTI dataset, which resulted in very high accuracy of poor image detection.

Additional efforts will be made to collect images with more diverse artifacts. Having a larger sample size will facilitate fine-tuning down to middle or lower layers in the deep neural network. Retraining from a very low layer may cause overfitting of training data, therefore, determination of which layer to retrain will be crucial to achieve an accurate and reproducible model.

The second step will be to establish a trustworthy gold standard for "good" images. The images can be first examined by the author and then validated by colleagues. As a final check, a radiologist who has expertise in DTI can examine the results and confirm labeling.

The third step will be to develop a multi-class classifier to categorize images according to artifact type. This work will allow images to be considered for further processing before an exclusion from subsequent analyses. A more diverse pool of corrupted images needs to be acquired, as mentioned above, to develop the multi-class classifier.

Lastly, it will be valuable to develop two versions of quality control tools and release them for public use. One version would be a generalized tool where the model is trained with data from different sites with different imaging parameters, so users can download the program and simply run it to test their diffusion images. The other version would be a site-specific tool, which generates higher detection accuracy for data from a specific site or center (similar to this work). Before assessing, users would need to download a pre-trained model and fine-tune it with their own dataset.

Eventually, the aforementioned DTI-based QC approaches will be extended to assessing 4-D raw DWI data. Considering that fitting a diffusion tensor does not necessarily require volumes with every diffusion-encoded direction (e.g., 30, 60), a few "poor" volumes (possibly due to a subject motion at a certain time) can be excluded, whereas the majority "good" volumes are kept.

REFERENCES

REFERENCES

[1] L. DePadilla, G. F. Miller, S. E. Jones, A. B. Peterson, and M. J. Breiding, "Self-Reported Concussions from Playing a Sport or Being Physically Active Among High School Students United States, 2017," The Centers for Disease Control and Prevention, Tech. Rep. 24, 6 2018.

[2] W. P. Meehan, III, R. C. Mannix, M. J. O'Brien, and M. W. Collins, "The Prevalence of Undiagnosed Concussions in Athletes," *Clinical journal of sport medicine : official journal of the Canadian Academy of Sport Medicine*, vol. 23, no. 5, p. 339, 9 2013.

[3] J. K. Register-Mihalik, L. A. Linnan, S. W. Marshall, T. C. V. McLeod, F. O. Mueller, and K. M. Guskiewicz, "Using theory to understand high school aged athletes intentions to report sport-related concussion: Implications for concussion education initiatives," *Brain Injury*, vol. 27, no. 7-8, pp. 878–886, 7 2013.

[4] T. B. Meier, B. J. Brummel, R. Singh, C. J. Nerio, D. W. Polanski, and P. S. Bellgowan, "The underreporting of self-reported symptoms following sports-related concussion," *Journal of Science and Medicine in Sport*, vol. 18, no. 5, pp. 507–511, 9 2015.

[5] A. K. Ommaya, L. Thibault, and F. A. Bandak, "Mechanisms of impact head injury," *International Journal of Impact Engineering*, vol. 15, no. 4, pp. 535–560, 8 1994.

[6] J. F. Geddes, G. H. Vowles, J. A. R. Nicoll, and T. Révész, "Neuronal cytoskeletal changes are an early consequence of repetitive head injury," *Acta Neuropathologica*, vol. 98, no. 2, pp. 171–178, 8 1999.

[7] B. I. Omalu, S. T. DeKosky, R. L. Hamilton, R. L. Minster, M. I. Kamboh, A. M. Shakir, and C. H. Wecht, "Chronic Traumatic Encephalopathy in a National Football League Player," *Neurosurgery*, vol. 59, no. 5, pp. 1086–1093, 2006.

[8] E. J. Lehman, M. J. Hein, S. L. Baron, and C. M. Gersic, "Neurodegenerative causes of death among retired National Football League players." *Neurology*, vol. 79, no. 19, pp. 1970–4, 2012.

[9] P. McCrory, N. Feddermann-Demont, J. Dvořák, J. D. Cassidy, A. McIntosh, P. E. Vos, R. J. Echemendia, W. Meeuwisse, and A. A. Tarnutzer, "What is the definition of sports-related concussion: a systematic review." *British journal of sports medicine*, vol. 51, no. 11, pp. 877–887, 6 2017.

[10] K. M. Guskiewicz, M. McCrea, S. W. Marshall, R. C. Cantu, C. Randolph, W. Barr, J. A. Onate, and J. P. Kelly, "Cumulative Effects Associated With Recurrent Concussion in Collegiate Football Players," *JAMA*, vol. 290, no. 19, p. 2549, 11 2003.

[11] A. C. McKee, R. C. Cantu, C. J. Nowinski, E. T. Hedley-Whyte, B. E. Gavett, A. E. Budson, V. E. Santini, H.-S. Lee, C. A. Kubilus, and R. A. Stern, "Chronic Traumatic Encephalopathy in Athletes: Progressive Tauopathy After Repetitive Head Injury," *Journal of Neuropathology & Experimental Neurology*, vol. 68, no. 7, pp. 709–735, 2009.

[12] B. Johnson, T. Neuberger, M. Gay, M. Hallett, and S. Slobounov, "Effects of Subconcussive Head Trauma on the Default Mode Network of the Brain," *Journal of Neurotrauma*, vol. 31, no. 23, pp. 1907–1913, 12 2014.

[13] T. M. Talavage, E. A. Nauman, E. L. Breedlove, U. Yoruk, A. E. Dye, K. E. Morigaki, H. Feuer, and L. J. Leverenz, "Functionally-Detected Cognitive Impairment in High School Football Players without Clinically-Diagnosed Concussion," *Journal of Neurotrauma*, vol. 31, no. 4, pp. 327–338, 2014.

[14] K. Abbas, T. E. Shenk, V. N. Poole, E. L. Breedlove, L. J. Leverenz, E. A. Nauman, T. M. Talavage, and M. E. Robinson, "Alteration of Default Mode Network in High School Football Athletes Due to Repetitive Subconcussive Mild Traumatic Brain Injury: A Resting-State Functional Magnetic Resonance Imaging Study," *Brain Connectivity*, vol. 5, no. 2, pp. 91–101, 2015.

[15] D. O. Svaldi, C. Joshi, M. E. Robinson, T. E. Shenk, K. Abbas, E. A. Nauman, L. J. Leverenz, and T. M. Talavage, "Cerebrovascular Reactivity Alterations in Asymptomatic High School Football Players," *Developmental Neuropsychology*, vol. 40, no. 2, pp. 80–84, 2015.

[16] T. W. McAllister, J. C. Ford, L. A. Flashman, A. Maerlender, R. M. Greenwald, J. G. Beckwith, R. P. Bolander, T. D. Tosteson, J. H. Turco, R. Raman, and S. Jain, "Effect of head impacts on diffusivity measures in a cohort of collegiate contact sport athletes." *Neurology*, vol. 82, no. 1, pp. 63–9, 2014.

[17] E. M. Davenport, C. T. Whitlow, J. E. Urban, M. A. Espeland, Y. Jung, D. A. Rosenbaum, G. A. Gioia, A. K. Powers, J. D. Stitzel, and J. A. Maldjian, "Abnormal White Matter Integrity Related to Head Impact Exposure in a Season of High School Varsity Football," *Journal of Neurotrauma*, vol. 31, no. 19, pp. 1617–1624, 2014.

[18] P. McCrory, W. H. Meeuwisse, M. Aubry, B. Cantu, J. Dvořák, R. J. Echemendia, L. Engebretsen, K. Johnston, J. S. Kutcher, M. Raftery, A. Sills, B. W. Benson, G. A. Davis, R. G. Ellenbogen, K. Guskiewicz, S. A. Herring, G. L. Iverson, B. D. Jordan, J. Kissick, M. McCrea, A. S. McIntosh, D. Maddocks, M. Makdissi, L. Purcell, M. Putukian, K. Schneider, C. H. Tator, and M. Turner, "Consensus statement on concussion in sport: the 4th International Conference on Concussion in Sport held in Zurich, November 2012," *British Journal of Sports Medicine*, vol. 47, no. 5, pp. 250–258, 4 2013.

[19] J. J. Bazarian, T. Zhu, B. Blyth, A. Borrino, and J. Zhong, "Subject-specific changes in brain white matter on diffusion tensor imaging after sports-related concussion," *Magnetic Resonance Imaging*, vol. 30, pp. 171–180, 2012.

[20] I. Y. Chun, X. Mao, E. L. Breedlove, L. J. Leverenz, E. A. Nauman, and T. M. Talavage, "DTI Detection of Longitudinal WM Abnormalities Due to Accumulated Head Impacts," *Developmental Neuropsychology*, vol. 40, no. 2, pp. 92–97, 2015.

[21] C. M. Baugh, E. Kroshus, D. H. Daneshvar, N. A. Filali, M. J. Hiscox, and L. H. Glantz, "Concussion Management in United States College Sports," *The American Journal of Sports Medicine*, vol. 43, no. 1, pp. 47–56, 1 2015.

[22] J. G. Beckwith, R. M. Greenwald, J. J. Chu, J. J. Crisco, S. Rowson, S. M. Duma, S. P. Broglio, T. W. McAllister, K. M. Guskiewicz, J. P. Mihalik, S. Anderson, B. Schnebel, P. G. Brolinson, and M. W. Collins, "Timing of Concussion Diagnosis is Related to Head Impact Exposure Prior to Injury," *Medicine and science in sports and exercise*, vol. 45, no. 4, p. 747, 4 2013.

[23] S. P. Broglio, J. J. Sosnoff, K. S. Rosengren, and K. McShane, "A Comparison of Balance Performance: Computerized Dynamic Posturography and a Random Motion Platform," *Archives of Physical Medicine and Rehabilitation*, vol. 90, no. 1, pp. 145–150, 2009.

[24] R. A. Stern, D. O. Riley, D. H. Daneshvar, C. J. Nowinski, R. C. Cantu, and A. C. McKee, "Long-term Consequences of Repetitive Brain Trauma: Chronic Traumatic Encephalopathy," *PM&R*, vol. 3, no. 10, pp. S460–S467, 2011.

[25] K. L. Kucera, R. K. Yau, J. Register-Mihalik, S. W. Marshall, L. C. Thomas, S. Wolf, R. C. Cantu, F. O. Mueller, and K. M. Guskiewicz, "Traumatic Brain and Spinal Cord Fatalities Among High School and College Football Players United States, 20052014," The Centers for Disease Control and Prevention, Tech. Rep. 52, 1 2017.

[26] P. J. Basser and D. K. Jones, "Diffusion-tensor MRI: theory, experimental design and data analysis - a technical review." *NMR in Biomedicine*, vol. 15, no. 7-8, pp. 456–467, 2002.

[27] C. Beaulieu, "The basis of anisotropic water diffusion in the nervous system - a technical review," *NMR in Biomedicine*, vol. 15, no. 7-8, pp. 435–455, 2002.

[28] J.-D. Tournier, S. Mori, and A. Leemans, "Diffusion tensor imaging and beyond." *Magnetic Resonance in Medicine*, vol. 65, no. 6, pp. 1532–1556, 6 2011.

[29] O. Dietrich, S. Heiland, and K. Sartor, "Noise correction for the exact determination of apparent diffusion coefficients at low SNR." *Magnetic Resonance in Medicine*, vol. 45, no. 3, pp. 448–453, 3 2001.

[30] A. Leemans and D. K. Jones, "The B-matrix must be rotated when correcting for subject motion in DTI data," *Magnetic Resonance in Medicine*, vol. 61, p. 13361349, 2009.

[31] D. R. Roalf, M. Quarmley, M. A. Elliott, T. D. Satterthwaite, S. N. Vandekar, K. Ruparel, E. D. Gennatas, M. E. Calkins, T. M. Moore, R. Hopson, K. Prabhakaran, C. T. Jackson, R. Verma, H. Hakonarson, R. C. Gur, and R. E. Gur, "The impact of quality assurance assessment on diffusion tensor imaging outcomes in a large-scale population-based cohort," *NeuroImage*, vol. 125, pp. 903–919, 2016.

[32] H. Jiang, P. C. M. van Zijl, J. Kim, G. D. Pearlson, and S. Mori, "DtiStudio: resource program for diffusion tensor computation and fiber bundle tracking." *Computer Methods and Programs in Biomedicine*, vol. 81, no. 2, pp. 106–116, 2 2006.

[33] C. B. Lauzon, A. J. Asman, M. L. Esparza, S. S. Burns, Q. Fan, Y. Gao, A. W. Anderson, N. Davis, L. E. Cutting, and B. A. Landman, "Simultaneous analysis and quality assurance for diffusion tensor imaging." *PloS one*, vol. 8, no. 4, p. e61737, 2013.

[34] I. Oguz, M. Farzinfar, J. Matsui, F. Budin, Z. Liu, G. Gerig, H. J. Johnson, and M. Styner, "DTIPrep: quality control of diffusion-weighted images." *Frontiers in Neuroinformatics*, vol. 8, p. 4, 2014.

[35] O. Esteban, D. Birman, M. Schaer, O. O. Koyejo, R. A. Poldrack, and K. J. Gorgolewski, "MRIQC: Predicting Quality in Manual MRI Assessment Protocols Using No-Reference Image Quality Measures," *bioRxiv*, p. 111294, 2 2017.

[36] F. Alfaro-Almagro, M. Jenkinson, N. K. Bangerter, J. L. Andersson, L. Griffanti, G. Douaud, S. N. Sotiropoulos, S. Jbabdi, M. Hernandez-Fernandez, E. Vallee, D. Vidaurre, M. Webster, P. McCarthy, C. Rorden, A. Daducci, D. C. Alexander, H. Zhang, I. Dragonu, P. M. Matthews, K. L. Miller, and S. M. Smith, "Image processing and Quality Control for the first 10,000 brain imaging datasets from UK Biobank," *NeuroImage*, vol. 166, pp. 400–424, 2 2018.

[37] I. Goodfellow, Y. Bengio, and A. Courville, *Deep learning.* MIT Press, 2016.

[38] L. Y. Pratt, "Discriminability-Based Transfer between Neural Networks," *Advances in neural information processing systems*, pp. 204–211, 1993.

[39] M. E. Robinson, E. R. Lindemer, J. R. Fonda, W. P. Milberg, R. E. McGlinchey, and D. H. Salat, "Close-range blast exposure is associated with altered functional connectivity in Veterans independent of concussion symptoms at time of exposure," *Human Brain Mapping*, vol. 36, no. 3, pp. 911–922, 2015.

[40] T. E. Shenk, M. E. Robinson, D. O. Svaldi, K. Abbas, K. M. Breedlove, L. J. Leverenz, E. A. Nauman, and T. M. Talavage, "fMRI of Visual Working Memory in High School Football Players," *Developmental Neuropsychology*, vol. 40, no. 2, pp. 63–68, 2015.

[41] K. Abbas, T. E. Shenk, V. N. Poole, M. E. Robinson, L. J. Leverenz, E. A. Nauman, and T. M. Talavage, "Effects of Repetitive Sub-Concussive Brain Injury on the Functional Connectivity of Default Mode Network in High School Football Athletes," *Developmental Neuropsychology*, vol. 40, no. 1, pp. 51–56, 2015.

[42] D. O. Svaldi, E. C. McCuen, C. Joshi, M. E. Robinson, Y. Nho, R. Hannemann, E. A. Nauman, L. J. Leverenz, and T. M. Talavage, "Cerebrovascular reactivity changes in asymptomatic female athletes attributable to high school soccer participation," *Brain Imaging and Behavior*, vol. 11, no. 1, pp. 98–112, 2017.

[43] D. O. Svaldi, C. Joshi, E. C. McCuen, J. P. Music, R. Hannemann, L. J. Leverenz, E. A. Nauman, and T. M. Talavage, "Accumulation of high magnitude acceleration events predicts cerebrovascular reactivity changes in female high school soccer athletes," *Brain Imaging and Behavior*, pp. 1–11, 2018.

[44] V. N. Poole, K. Abbas, T. E. Shenk, E. L. Breedlove, K. M. Breedlove, M. E. Robinson, L. J. Leverenz, E. A. Nauman, T. M. Talavage, and U. Dydak, "MR Spectroscopic Evidence of Brain Injury in the Non-Diagnosed Collision Sport Athlete," *Developmental Neuropsychology*, vol. 39, no. 6, pp. 459–473, 2014.

[45] V. N. Poole, E. L. Breedlove, T. E. Shenk, K. Abbas, M. E. Robinson, L. J. Leverenz, E. A. Nauman, U. Dydak, and T. M. Talavage, "Sub-Concussive Hit Characteristics Predict Deviant Brain Metabolism in Football Athletes," *Developmental Neuropsychology*, vol. 40, no. 1, pp. 12–17, 2015.

[46] S. Bari, D. O. Svaldi, I. Jang, T. E. Shenk, V. N. Poole, T. Lee, U. Dydak, J. V. Rispoli, E. A. Nauman, and T. M. Talavage, "Dependence on subconcussive impacts of brain metabolism in collision sport athletes: an MR spectroscopic study," *Brain Imaging and Behavior*, pp. 1–15, 2018.

[47] S. M. Slobounov, A. Walter, H. C. Breiter, D. C. Zhu, X. Bai, T. Bream, P. Seidenberg, X. Mao, B. Johnson, and T. M. Talavage, "The effect of repetitive subconcussive collisions on brain integrity in collegiate football players over a single football season: A multi-modal neuroimaging study," *NeuroImage: Clinical*, vol. 14, pp. 708–718, 2017.

[48] T. M. Talavage, E. A. Nauman, and L. J. Leverenz, "The Role of Medical Imaging in the Recharacterization of Mild Traumatic Brain Injury Using Youth Sports as a Laboratory," *Frontiers in Neurology*, vol. 6, p. 273, 2016.

[49] C. Beaulieu, "The basis of anisotropic water diffusion in the nervous system - a technical review," *NMR in Biomedicine*, vol. 15, no. 7-8, pp. 435–455, 11 2002.

[50] K. Arfanakis, V. M. Haughton, J. D. Carew, B. P. Rogers, R. J. Dempsey, and E. Meyerand, "Diffusion Tensor MR Imaging in Diffuse Axonal Injury," *American Journal of Neuroradiology*, vol. 23, pp. 794–802, 2002.

[51] M. Inglese, S. Makani, G. Johnson, B. A. Cohen, J. A. Silver, O. Gonen, and R. I. Grossman, "Diffuse axonal injury in mild traumatic brain injury: a diffusion tensor imaging study," *Journal of Neurosurgery*, vol. 103, no. 2, pp. 298–303, 2005.

[52] J. J. Bazarian, J. Zhong, B. Blyth, T. Zhu, V. Kavcic, and D. Peterson, "Diffusion Tensor Imaging Detects Clinically Important Axonal Damage after Mild Traumatic Brain Injury: A Pilot Study," *Journal of Neurotrauma*, vol. 24, pp. 1447–1459, 2007.

[53] I. K. Koerte, D. Kaufmann, E. Hartl, S. Bouix, O. Pasternak, M. Kubicki, A. Rauscher, D. K. B. Li, S. B. Dadachanji, J. A. Taunton, L. A. Forwell, A. M. Johnson, P. S. Echlin, and M. E. Shenton, "A prospective study of physician-observed concussion during a varsity university hockey season: white matter integrity in ice hockey players. Part 3 of 4," *Neurosurgical Focus*, vol. 33, no. 6, p. E3, 2012.

[54] M. C. Mayinger, K. Merchant-Borna, J. Hufschmidt, M. Muehlmann, I. R. Weir, B.-S. Rauchmann, M. E. Shenton, I. K. Koerte, and J. J. Bazarian, "White matter alterations in college football players: a longitudinal diffusion tensor imaging study," *Brain Imaging and Behavior*, vol. 12, no. 1, pp. 44–53, 2018.

[55] G. D. Myer, W. Yuan, K. D. B. Foss, S. Thomas, D. Smith, J. Leach, A. W. Kiefer, C. Dicesare, J. Adams, P. J. Gubanich, K. Kitchen, D. K. Schneider, D. Braswell, D. Krueger, and M. Altaye, "Analysis of head impact exposure and brain microstructure response in a season-long application of a jugular

vein compression collar: a prospective, neuroimaging investigation in American football," *British Journal of Sports Medicine*, vol. 50, no. 20, pp. 1276–1285, 2016.

[56] W. Yuan, K. D. Barber Foss, S. Thomas, C. A. DiCesare, J. A. Dudley, K. Kitchen, B. Gadd, J. L. Leach, D. Smith, M. Altaye, P. Gubanich, R. T. Galloway, P. McCrory, J. E. Bailes, R. Mannix, W. P. Meehan, and G. D. Myer, "White matter alterations over the course of two consecutive high-school football seasons and the effect of a jugular compression collar: A preliminary longitudinal diffusion tensor imaging study," *Human Brain Mapping*, vol. 39, no. 1, pp. 491–508, 2018.

[57] J. J. Bazarian, T. Zhu, J. Zhong, D. Janigro, E. Rozen, A. Roberts, H. Javien, K. Merchant-Borna, B. Abar, and E. G. Blackman, "Persistent, Long-term Cerebral White Matter Changes after Sports-Related Repetitive Head Impacts," *PLoS ONE*, vol. 9, no. 4, p. e94734, 2014.

[58] M. L. Lipton, N. Kim, M. E. Zimmerman, M. Kim, W. F. Stewart, C. A. Branch, and R. B. Lipton, "Soccer Heading Is Associated with White Matter Microstructural and Cognitive Abnormalities," *Radiology*, vol. 268, no. 3, pp. 850–857, 2013.

[59] N.-J. Gong, S. Kuzminski, M. Clark, M. Fraser, M. Sundman, K. Guskiewicz, J. R. Petrella, and C. Liu, "Microstructural alterations of cortical and deep gray matter over a season of high school football revealed by diffusion kurtosis imaging," *Neurobiology of Disease*, vol. 119, pp. 79–87, 2018.

[60] G. D. Myer, K. Barber Foss, S. Thomas, R. Galloway, C. A. Dicesare, J. Dudley, B. Gadd, J. Leach, D. Smith, P. Gubanich, W. P. Meehan, M. Altaye, P. Lavin, and W. Yuan, "Altered brain microstructure in association with repetitive sub-concussive head impacts and the potential protective effect of jugular vein compression: A longitudinal study of female soccer athletes," *British Journal of Sports Medicine*, vol. 0, pp. 1–14, 2018.

[61] L. Miles, R. I. Grossman, G. Johnson, J. S. Babb, L. Diller, and M. Inglese, "Short-term DTI predictors of cognitive dysfunction in mild traumatic brain injury," *Brain Injury*, vol. 22, no. 2, pp. 115–122, 2008.

[62] V. A. Cubon, M. Putukian, C. Boyer, and A. Dettwiler, "A Diffusion Tensor Imaging Study on the White Matter Skeleton in Individuals with Sports-Related Concussion," *Journal of Neurotrauma*, vol. 28, no. 2, pp. 189–201, 2011.

[63] S. M. Mustafi, J. Harezlak, K. M. Koch, A. S. Nencka, T. B. Meier, J. D. West, C. C. Giza, J. P. DiFiori, K. M. Guskiewicz, J. P. Mihalik, S. M. LaConte, S. M. Duma, S. P. Broglio, A. J. Saykin, M. McCrea, T. W. McAllister, and Y.-C. Wu, "Acute White-Matter Abnormalities in Sports-Related Concussion: A Diffusion Tensor Imaging Study from the NCAA-DoD CARE Consortium," *Journal of Neurotrauma*, vol. 35, no. 22, pp. 2653–2664, 2018.

[64] T. W. McAllister, J. C. Ford, S. Ji, J. G. Beckwith, L. A. Flashman, K. Paulsen, and R. M. Greenwald, "Maximum Principal Strain and Strain Rate Associated with Concussion Diagnosis Correlates with Changes in Corpus Callosum White Matter Indices," *Annals of Biomedical Engineering*, vol. 40, no. 1, pp. 127–140, 2012.

[65] E. A. Wilde, S. R. Mccauley, J. V. Hunter, E. D. Bigler, Z. Chu, Z. J. Wang, G. R. Hanten, M. Troyanskaya, R. Yallampalli, B. X. Li, J. Chia, and H. S. Levin, "Diffusion tensor imaging of acute mild traumatic brain injury in adolescents," *Neurology*, vol. 70, pp. 948–955, 2008.

[66] L. C. Henry, J. Tremblay, S. Tremblay, A. Lee, C. Brun, N. Lepore, H. Theoret, D. Ellemberg, and M. Lassonde, "Acute and Chronic Changes in Diffusivity Measures after Sports Concussion," *Journal of Neurotrauma*, vol. 28, no. 10, pp. 2049–2059, 2011.

[67] A. R. Mayer, J. M. Ling, Z. Yang, A. Pena, R. A. Yeo, and S. Klimaj, "Diffusion abnormalities in pediatric mild traumatic brain injury," *The Journal of neuroscience : the official journal of the Society for Neuroscience*, vol. 32, no. 50, pp. 17 961–9, 2012.

[68] A. R. Mayer, J. Ling, M. V. Mannell, C. Gasparovic, J. P. Phillips, D. Doezema, R. Reichard, and R. A. Yeo, "A prospective diffusion tensor imaging study in mild traumatic brain injury." *Neurology*, vol. 74, no. 8, pp. 643–50, 2010.

[69] Z. Chu, E. A. Wilde, J. V. Hunter, S. R. McCauley, E. D. Bigler, M. Troyanskaya, R. Yallampalli, J. M. Chia, and H. S. Levin, "Voxel-based analysis of diffusion tensor imaging in mild traumatic brain injury in adolescents." *AJNR. American journal of neuroradiology*, vol. 31, no. 2, pp. 340–6, 2010.

[70] J. M. Ling, A. Peña, R. A. Yeo, F. L. Merideth, S. Klimaj, C. Gasparovic, and A. R. Mayer, "Biomarkers of increased diffusion anisotropy in semi-acute mild traumatic brain injury: a longitudinal perspective," *Brain*, vol. 135, no. 4, pp. 1281–1292, 2012.

[71] J. T. Povlishock and D. I. Katz, "Update of Neuropathology and Neurological Recovery After Traumatic Brain Injury," *Journal of Head Trauma Rehabilitation*, vol. 20, no. 1, pp. 76–94, 2005.

[72] M. F. Kraus, T. Susmaras, B. P. Caughlin, C. J. Walker, J. A. Sweeney, and D. M. Little, "White matter integrity and cognition in chronic traumatic brain injury: a diffusion tensor imaging study," *Brain*, vol. 130, pp. 2508–2519, 2007.

[73] M. L. Lipton, E. Gellella, C. Lo, T. Gold, B. A. Ardekani, K. Shifteh, J. A. Bello, and C. A. Branch, "Multifocal White Matter Ultrastructural Abnormalities in Mild Traumatic Brain Injury with Cognitive Disability: A Voxel-Wise Analysis of Diffusion Tensor Imaging," *Journal of Neurotrauma*, vol. 25, pp. 1335–1342, 2008.

[74] E. L. Breedlove, M. Robinson, T. M. Talavage, K. E. Morigaki, U. Yoruk, K. O'Keefe, J. King, L. J. Leverenz, J. W. Gilger, and E. A. Nauman, "Biomechanical correlates of symptomatic and asymptomatic neurophysiological impairment in high school football," *Journal of Biomechanics*, vol. 45, no. 7, pp. 1265–1272, 2012.

[75] E. McCuen, D. Svaldi, K. Breedlove, N. Kraz, B. Cummiskey, E. L. Breedlove, J. Traver, K. F. Desmond, R. E. Hannemann, E. Zanath, A. Guerra, L. Leverenz, T. M. Talavage, and E. A. Nauman, "Collegiate women's soccer players suffer greater cumulative head impacts than their high school counterparts," *Journal of Biomechanics*, vol. 48, no. 13, pp. 3720–3723, 2015.

[76] B. Cummiskey, D. Schiffmiller, T. M. Talavage, L. Leverenz, J. J. Meyer, D. Adams, and E. A. Nauman, "Reliability and accuracy of helmet-mounted and head-mounted devices used to measure head accelerations," *Proceedings of the Institution of Mechanical Engineers, Part P: Journal of Sports Engineering and Technology*, vol. 231, no. 2, pp. 144–153, 2017.

[77] R. Jadischke, D. C. Viano, N. Dau, A. I. King, and J. McCarthy, "On the accuracy of the Head Impact Telemetry (HIT) System used in football helmets," *Journal of Biomechanics*, vol. 46, no. 13, pp. 2310–2315, 2013.

[78] S. M. Smith, M. Jenkinson, M. W. Woolrich, C. F. Beckmann, T. E. J. Behrens, H. Johansen-Berg, P. R. Bannister, M. De Luca, I. Drobnjak, D. E. Flitney, R. K. Niazy, J. Saunders, J. Vickers, Y. Zhang, N. De Stefano, J. M. Brady, and P. M. Matthews, "Advances in functional and structural MR image analysis and implementation as FSL," *NeuroImage*, vol. 23, p. S208S219, 2004.

[79] M. Jenkinson, C. F. Beckmann, T. E. J. Behrens, M. W. Woolrich, and S. M. Smith, "FSL," *NeuroImage*, vol. 62, pp. 782–790, 2012.

[80] M. W. Woolrich, S. Jbabdi, B. Patenaude, M. Chappell, S. Makni, T. Behrens, C. Beckmann, M. Jenkinson, and S. M. Smith, "Bayesian analysis of neuroimaging data in FSL," *NeuroImage*, vol. 45, no. 1, pp. S173–S186, 2009.

[81] S. M. Smith, "Fast robust automated brain extraction," *Human Brain Mapping*, vol. 17, no. 3, pp. 143–155, 2002.

[82] J. L. Andersson, M. S. Graham, E. Zsoldos, and S. N. Sotiropoulos, "Incorporating outlier detection and replacement into a non-parametric framework for movement and distortion correction of diffusion MR images," *NeuroImage*, vol. 141, pp. 556–572, 2016.

[83] J. L. Andersson and S. N. Sotiropoulos, "An integrated approach to correction for off-resonance effects and subject movement in diffusion MR imaging," *NeuroImage*, vol. 125, pp. 1063–1078, 2016.

[84] T. Behrens, M. Woolrich, M. Jenkinson, H. Johansen-Berg, R. Nunes, S. Clare, P. Matthews, J. Brady, and S. Smith, "Characterization and propagation of uncertainty in diffusion-weighted MR imaging," *Magnetic Resonance in Medicine*, vol. 50, no. 5, pp. 1077–1088, 2003.

[85] M. Murugavel, V. Cubon, M. Putukian, R. Echemendia, J. Cabrera, D. Osherson, and A. Dettwiler, "A Longitudinal Diffusion Tensor Imaging Study Assessing White Matter Fiber Tracts after Sports-Related Concussion," *Journal of Neurotrauma*, vol. 31, no. 22, pp. 1860–1871, 2014.

[86] J. Ling, F. Merideth, A. Caprihan, A. Pena, T. Teshiba, and A. R. Mayer, "Head injury or head motion? Assessment and quantification of motion artifacts in diffusion tensor imaging studies," *Human Brain Mapping*, vol. 33, no. 1, pp. 50–62, 2012.

[87] J. L. R. Andersson, M. Jenkinson, and S. M. Smith, "Non-linear optimisation. FMRIB technical report TR07JA1," FMRIB Centre, Tech. Rep. June, 2007.

[88] J. L. R. Andersson, M. Jenkinson, and S. Smith, "Non-linear registration aka Spatial normalisation FMRIB Technial Report TR07JA2," FMRIB Centre, Tech. Rep., 2007.

[89] S. M. Smith, M. Jenkinson, M. W. Woolrich, C. F. Beckmann, T. E. Behrens, H. Johansen-Berg, P. R. Bannister, M. De Luca, I. Drobnjak, D. E. Flitney, R. K. Niazy, J. Saunders, J. Vickers, Y. Zhang, N. De Stefano, J. M. Brady, and P. M. Matthews, "Advances in functional and structural MR image analysis and implementation as FSL," *NeuroImage*, vol. 23, pp. S208–S219, 2004.

[90] S. M. Smith, M. Jenkinson, H. Johansen-Berg, D. Rueckert, T. E. Nichols, C. E. Mackay, K. E. Watkins, O. Ciccarelli, M. Z. Cader, P. M. Matthews, and T. E. Behrens, "Tract-based spatial statistics: Voxelwise analysis of multi-subject diffusion data," *NeuroImage*, vol. 31, no. 4, pp. 1487–1505, 2006.

[91] S. M. Smith and T. E. Nichols, "Threshold-free cluster enhancement: Addressing problems of smoothing, threshold dependence and localisation in cluster inference," *NeuroImage*, vol. 44, no. 1, pp. 83–98, 2009.

[92] S. Mori, S. Wakana, P. C. Van Zijl, and L. M. Nagae-Poetscher, *MRI Atlas of Human White Matter*, 1st ed. San Diego: Elsevier, 2005.

[93] U. C. Wieshmann, C. A. Clark, M. R. Symms, F. Franconi, G. J. Barker, and S. D. Shorvon, "Reduced Anisotropy of Water Diffusion in Structural Cerebral Abnormalities Demonstrated with Diffusion Tensor Imaging," *Magnetic Resonance Imaging*, vol. 17, no. 9, pp. 1269–1274, 1999.

[94] J. M. Stamm, A. P. Bourlas, C. M. Baugh, N. G. Fritts, D. H. Daneshvar, B. M. Martin, M. D. McClean, Y. Tripodis, and R. A. Stern, "Age of first exposure to football and later-life cognitive impairment in former NFL players." *Neurology*, vol. 84, no. 11, pp. 1114–20, 2015.

[95] M. Marar, N. M. McIlvain, S. K. Fields, and R. D. Comstock, "Epidemiology of Concussions Among United States High School Athletes in 20 Sports," *The American Journal of Sports Medicine*, vol. 40, no. 4, pp. 747–755, 2012.

[96] K. Y. Manning, A. Schranz, R. Bartha, G. A. Dekaban, C. Barreira, A. Brown, L. Fischer, K. Asem, T. J. Doherty, D. D. Fraser, J. Holmes, and R. S. Menon, "Multiparametric MRI changes persist beyond recovery in concussed adolescent hockey players," *Neurology*, vol. 89, no. 21, pp. 2157–2166, 2017.

[97] D. N. Pandya, "The topography of commissural fibers." *Two hemispheres-one brain: Functions of the corpus callosum*, pp. 47–73, 1986.

[98] C. Njiokiktjien, L. de Sonneville, and J. Vaal, "Callosal size in children with learning disabilities," *Behavioural Brain Research*, vol. 64, no. 1-2, pp. 213–218, 1994.

[99] W. S. Brown, M. A. Jeeves, R. Dietrich, and D. S. Burnison, "Bilateral field advantage and evoked potential interhemispheric transmission in commissurotomy and callosal agenesis," *Neuropsychologia*, vol. 37, no. 10, pp. 1165–1180, 1999.

[100] J. C. Eliassen, K. Baynes, and M. S. Gazzaniga, "Direction information coordinated via the posterior third of the corpus callosum during bimanual movements," *Experimental Brain Research*, vol. 128, no. 4, pp. 573–577, 1999.

[101] C. R. McDonald, B. Crosson, E. Valenstein, and D. Bowers, "Verbal Encoding Deficits in a Patient with a Left Retrosplenial Lesion," *Neurocase*, vol. 7, no. 5, pp. 407–417, 2001.

[102] F. Tomaiuolo, U. Nocentini, L. Grammaldo, and C. Caltagirone, "Interhemispheric transfer time in a patient with a partial lesion of the corpus callosum," *Neuroreport*, vol. 12, no. 7, pp. 1469–1472, 2001.

[103] F. L. Bookstein, A. P. Streissguth, P. D. Sampson, P. D. Connor, and H. M. Barr, "Corpus Callosum Shape and Neuropsychological Deficits in Adult Males with Heavy Fetal Alcohol Exposure," *NeuroImage*, vol. 15, no. 1, pp. 233–251, 2002.

[104] A. A. Dorion, M. Sarazin, D. Hasboun, V. Hahn-Barma, B. Dubois, A. Zouaoui, C. Marsault, and M. Duyme, "Relationship between attentional performance and corpus callosum morphometry in patients with Alzheimers disease," *Neuropsychologia*, vol. 40, no. 7, pp. 946–956, 2002.

[105] F. Hoeft, N. Barnea-Goraly, B. W. Haas, G. Golarai, D. Ng, D. Mills, J. Korenberg, U. Bellugi, A. Galaburda, and A. L. Reiss, "More is not always better: increased fractional anisotropy of superior longitudinal fasciculus associated with poor visuospatial abilities in Williams syndrome." *The Journal of neuroscience : the official journal of the Society for Neuroscience*, vol. 27, no. 44, pp. 11 960–5, 2007.

[106] B. D. Peters, P. R. Szeszko, J. Radua, T. Ikuta, P. Gruner, P. DeRosse, J. Zhang, A. Giorgio, D. Qiu, S. F. Tapert, J. Brauer, M. R. Asato, P. L. Khong, A. C. James, J. A. Gallego, and A. K. Malhotra, "White Matter Development in Adolescence: Diffusion Tensor Imaging and Meta-Analytic Results," *Schizophrenia Bulletin*, vol. 38, no. 6, pp. 1308–1317, 2012.

[107] R. E. Frye, K. Hasan, B. Malmberg, L. Desouza, P. Swank, K. Smith, and S. Landry, "Superior longitudinal fasciculus and cognitive dysfunction in adolescents born preterm and at term," *Developmental Medicine & Child Neurology*, vol. 52, no. 8, pp. 760–766, 2010.

[108] D. E. Haines, *Neuroanatomy: An Atlas of Structures, Sections, and Systems*. Lippincott Williams & Wilkins, 2004.

[109] S. Lehéricy, M. Ducros, P.-F. Van De Moortele, C. Francois, L. Thivard, C. Poupon, N. Swindale, K. Ugurbil, and D.-S. Kim, "Diffusion tensor fiber tracking shows distinct corticostriatal circuits in humans," *Annals of Neurology*, vol. 55, no. 4, pp. 522–529, 2004.

[110] M. D. Greicius, K. Supekar, V. Menon, and R. F. Dougherty, "Resting-State Functional Connectivity Reflects Structural Connectivity in the Default Mode Network," *Cerebral Cortex*, vol. 19, no. 1, pp. 72–78, 2009.

[111] M. v. d. Heuvel, R. Mandl, J. Luigjes, and H. H. Pol, "Microstructural Organization of the Cingulum Tract and the Level of Default Mode Functional Connectivity," *Journal of Neuroscience*, vol. 28, no. 43, pp. 10 844–10 851, 2008.

[112] O. Devinsky, M. J. Morrell, and B. A. Vogt, "Contributions of anterior cingulate cortex to behaviour," *Brain*, vol. 118, no. 1, pp. 279–306, 1995.

[113] J. M. Allman, A. Hakeem, J. M. Erwin, E. Nimchinsky, and P. Hof, "The Anterior Cingulate Cortex," *Annals of the New York Academy of Sciences*, vol. 935, no. 1, pp. 107–117, 2006.

[114] P. Brodal, *The Central Nervous System: Structure and Function.* Oxford University Press, 2004.

[115] A. Büki and J. T. Povlishock, "All roads lead to disconnection? Traumatic axonal injury revisited," *Acta Neurochirurgica*, vol. 148, no. 2, pp. 181–194, 2006.

[116] L. Conforti, J. Gilley, and M. P. Coleman, "Wallerian degeneration: an emerging axon death pathway linking injury and disease," *Nature Reviews Neuroscience*, vol. 15, no. 6, pp. 394–409, 2014.

[117] W. L. Maxwell, E. Bartlett, and H. Morgan, "Wallerian Degeneration in the Optic Nerve Stretch-Injury Model of Traumatic Brain Injury: A Stereological Analysis," *Journal of Neurotrauma*, vol. 32, no. 11, pp. 780–790, 2015.

[118] A. G. Gross, "A New Theory on the Dynamics of Brain Concussion and Brain Injury," *Journal of Neurosurgery*, vol. 15, no. 5, pp. 548–561, 1958.

[119] P. J. McMahon, A. Hricik, J. K. Yue, A. M. Puccio, T. Inoue, H. F. Lingsma, S. R. Beers, W. A. Gordon, A. B. Valadka, G. T. Manley, Okonkwo, D. O. the TRACK-TBI investiga, S. S. Casey, S. R. Cooper, K. Dams-O'Connor, D. K. Menon, M. D. Sorani, E. L. Yuh, P. Mukherjee, D. M. Schnyer, and M. J. Vassar, "Symptomatology and Functional Outcome in Mild Traumatic Brain Injury: Results from the Prospective TRACK-TBI Study," *Journal of Neurotrauma*, vol. 31, no. 1, pp. 26–33, 2014.

[120] E. Evans, D. Asuzu, N. E. Cook, P. Caruso, E. Townsend, B. Costine-Bartell, C. Fortes-Monteiro, G. Hotz, A.-C. Duhaime, D. Ramon, G. Joseph, M. Geoff, M. Pratik, O. David, R. Claudia, and T. Nancy, "Traumatic Brain Injury-Related Symptoms Reported by Parents: Clinical, Imaging, and Host Predictors in Children with Impairments in Consciousness Less than 24 Hours," *Journal of Neurotrauma*, vol. 35, no. 19, pp. 2287–2297, 2018.

[121] P. S. Auerbach and W. H. Waggoner, "Its Time to Change the Rules," *JAMA*, vol. 316, no. 12, pp. 1260–1261, 2016.

[122] A. Marmarou, S. Signoretti, P. P. Fatouros, G. Portella, G. A. Aygok, and M. R. Bullock, "Predominance of cellular edema in traumatic brain swelling in patients with severe head injuries," *Journal of Neurosurgery*, vol. 104, no. 5, pp. 720–730, 2006.

[123] J. A. Barkovich, "Concepts of Myelin and Myelination in Neuroradiology," *American Journal of Neuroradiology*, vol. 21, no. 6, pp. 1099–1109, 2000.

[124] J. L. Lancaster, T. Andrews, L. J. Hardies, S. Dodd, and P. T. Fox, "Three-pool model of white matter," *Journal of Magnetic Resonance Imaging*, vol. 17, no. 1, pp. 1–10, 2003.

[125] C. H. Sotak, "Nuclear magnetic resonance (NMR) measurement of the apparent diffusion coefficient (ADC) of tissue water and its relationship to cell volume changes in pathological states," *Neurochemistry International*, vol. 45, no. 4, pp. 569–582, 2004.

[126] S. M. Babb, Y. Ke, N. Lange, M. J. Kaufman, P. F. Renshaw, and B. M. Cohen, "Oral choline increases choline metabolites in human brain," *Psychiatry Research: Neuroimaging*, vol. 130, no. 1, pp. 1–9, 2004.

[127] P. Dechent, P. J. W. Pouwels, B. Wilken, F. Hanefeld, and J. Frahm, "Increase of total creatine in human brain after oral supplementation of creatine-monohydrate," *American Journal of Physiology-Regulatory, Integrative and Comparative Physiology*, vol. 277, no. 3, pp. R698–R704, 1999.

[128] J. Tan, S. Bluml, T. Hoang, D. Dubowitz, G. Mevenkamp, and B. Ross, "Lack of effect of oral choline supplement on the concentrations of choline metabolites in human brain," *Magnetic Resonance in Medicine*, vol. 39, no. 6, pp. 1005–1010, 1998.

[129] R. J. Maddock, G. A. Casazza, M. H. Buonocore, and C. Tanase, "Vigorous exercise increases brain lactate and Glx (glutamate + glutamine): A dynamic 1H-MRS study," *NeuroImage*, vol. 57, no. 4, pp. 1324–1330, 2011.

[130] C. Lebel and C. Beaulieu, "Longitudinal Development of Human Brain Wiring Continues from Childhood into Adulthood," *Journal of Neuroscience*, vol. 31, no. 30, pp. 10 937–10 947, 2011.

[131] C. Lebel, M. Gee, R. Camicioli, M. Wieler, W. Martin, and C. Beaulieu, "Diffusion tensor imaging of white matter tract evolution over the lifespan," *NeuroImage*, vol. 60, no. 1, pp. 340–352, 2012.

[132] A. Giorgio, K. Watkins, M. Chadwick, S. James, L. Winmill, G. Douaud, N. De Stefano, P. Matthews, S. Smith, H. Johansen-Berg, and A. James, "Longitudinal changes in grey and white matter during adolescence," *NeuroImage*, vol. 49, no. 1, pp. 94–103, 2010.

[133] D. J. Simmonds, M. N. Hallquist, M. Asato, and B. Luna, "Developmental stages and sex differences of white matter and behavioral development through adolescence: A longitudinal diffusion tensor imaging (DTI) study," *NeuroImage*, vol. 92, pp. 356–368, 2014.

[134] S. Mori and J.-D. Tournier, *Introduction to Diffusion Tensor Imaging: and Higher Order Models*, 2nd ed. San Diego: Academic Press, 2013.

[135] Z. Liu, Y. Wang, G. Gerig, S. Gouttard, R. Tao, T. Fletcher, and M. Styner, "Quality control of diffusion weighted images," in *Proceedings of the International Society for Optical Engineering*, B. J. Liu and W. W. Boonn, Eds., vol. 7628. International Society for Optics and Photonics, 3 2010, p. 76280J.

[136] J. E. Iglesias, G. Lerma-Usabiaga, L. C. Garcia-Peraza-Herrera, S. Martinez, and P. M. Paz-Alonso, "Retrospective Head Motion Estimation in Structural Brain MRI with 3D CNNs," in *Medical Image Computing and Computer-Assisted Intervention*. Springer, Cham, 2017, pp. 314–322.

[137] C. Kelly, M. Pietsch, S. Counsell, and J.-D. Tournier, "Transfer learning and convolutional neural net fusion for motion artefact detection," in *Proceedings of the Annual Meeting of the International Society for Magnetic Resonance in Medicine*, Honolulu, Hawaii, 2017, p. 3523.

[138] M. S. Graham, I. Drobnjak, and H. Zhang, "A supervised learning approach for diffusion MRI quality control with minimal training data," *NeuroImage*, vol. 178, pp. 668–676, 9 2018.

[139] C. Rorden and M. Brett, "Stereotaxic Display of Brain Lesions," *Behavioural Neurology*, vol. 12, no. 4, pp. 191–200, 2000.

[140] O. Russakovsky, J. Deng, H. Su, J. Krause, S. Satheesh, S. Ma, Z. Huang, A. Karpathy, A. Khosla, M. Bernstein, A. C. Berg, and L. Fei-Fei, "ImageNet Large Scale Visual Recognition Challenge," *International Journal of Computer Vision*, vol. 115, pp. 211–252, 2015.

[141] M. D. Zeiler, "ADADELTA: An Adaptive Learning Rate Method," *arXiv preprint*, vol. 1212, no. 5701, 12 2012.

[142] F. Chollet, "Keras," 2015.

[143] M. Abadi, A. Agarwal, P. Barham, E. Brevdo, Z. Chen, C. Citro, G. S. Corrado, A. Davis, J. Dean, M. Devin, S. Ghemawat, I. Goodfellow, A. Harp, G. Irving, M. Isard, Y. Jia, R. Jozefowicz, L. Kaiser, M. Kudlur, J. Levenberg, D. Mané, R. Monga, S. Moore, D. Murray, C. Olah, M. Schuster, J. Shlens, B. Steiner, I. Sutskever, K. Talwar, P. Tucker, V. Vanhoucke, V. Vasudevan, F. Viégas, O. Vinyals, P. Warden, M. Wattenberg, M. Wicke, Y. Yu, X. Zheng, and G. Research, "TensorFlow: Large-Scale Machine Learning on Heterogeneous Distributed Systems," *arXiv preprint*, vol. 1603.04467, 2016.

[144] J. Nickolls, I. Buck, M. Garland, and K. Skadron, "Scalable parallel programming with CUDA," p. 40, 3 2008.

[145] S. Chetlur, C. Woolley, P. Vandermersch, J. Cohen, J. Tran, B. Catanzaro, and E. Shelhamer, "cuDNN: Efficient Primitives for Deep Learning," *arXiv preprint*, 10 2014.

[146] F. Pedregosa, G. Varoquaux, A. Gramfort, V. Michel, B. Thirion, O. Grisel, M. Blondel, P. Prettenhofer, R. Weiss, V. Dubourg, J. Vanderplas, A. Passos, D. Cournapeau, M. Brucher, M. Perrot, and . Duchesnay, "Scikit-learn: Machine Learning in Python," *Journal of Machine Learning Research*, vol. 12, no. Oct, pp. 2825–2830, 2011.

[147] I. Jang, S. Bari, Y. Zou, N. L. Vike, P. Kashyap, and T. M. Talavage, "Test-Retest and Between-Site Reliability in a Multisite Diffusion Tensor Imaging Study," in *Proceedings of International Society for Magnetic Resonance in Medicine*, vol. 3239, Paris, France, 2018.

[148] I. Jang, Y. Zou, V. N. Poole, and T. M. Talavage, "Journal of neurotrauma." *Journal of neurotrauma*, vol. 35, no. 16, p. A116, 2018.

[149] I. Jang, S. Bari, E. A. Nauman, and T. M. Talavage, "Predictor Identification for White Matter Integrity in Football Athletes using Stepwise Regression," in *Proceedings of the Organization for Human Brain Mapping*, 2017, p. 1393.

VITA

VITA

Keywords: Neuroimaging | Traumatic Brain Injury | Machine Learning | Image Processing

---

Education

Purdue University	West Lafayette, IN
Ph.D. & M.S. in Electrical and Computer Engineering – GPA: 3.6/4.0;	*Aug 2013 – Present*

- Dissertation title: Diffusion Tensor Imaging Analysis for Subconcussive Trauma in Football and Convolutional Neural Network-Based Image Quality Control That Does Not Require a Big Dataset
- Committee: Profs. Thomas Talavage, Edward Delp, Eric Nauman, and Michael Zoltowski

Yonsei University	Seoul, South Korea
B.S. in Electrical and Electronics Engineering – GPA: 3.8/4.0; Honors Student Awards (three times)	*Mar 2007 – Feb 2013*

Academic Research Experience

Purdue University	West Lafayette, IN
Research – *academic advisor: Prof. Thomas Talavage*	*Aug 2013 – Present*

- Skills: Neuroimaging (diffusion MRI, functional MRI, T1w, EEG, NIRS), Image Processing, Statistical Testing, Machine Learning (Deep learning, Transfer learning, Boosting, Random forest, Support vector machine, Regression analysis, Bayesian classification, Principal component analysis, kNN, Manifold learning, Clustering)
- Dissertation Topics: 1) Characterization of effects of repetitive head impact exposure on white matter diffusivity or integrity in high school football athletes using diffusion tensor imaging. 2) Automated quality assessment of diffusion-weighted MR images with convolutional neural networks and transfer learning.
- Past Projects' Keywords: resting-state fMRI, cerebrovascular reactivity, parallel transmit/receive SENSE MRI.

Research Assistant – *Prof. Anne Sereno*   *Jan 2019 – Present*

- Project1: Identifying differences between various deep learning models (e.g., Faster R-CNN, YOLO, SSD) and general principles of neural processing in the brain, ranging from pooling rules and local connectivity to architecture (e.g., the brain has multiple, somewhat separable cortical streams with different functionalities). Discovering how specific changes alter performance in identification and localization of objects.
- Responsibility1: Neural network modeling and implementation
- Project2: Characterization of behavioral effects of repetitive head impact exposure using tablet-based tasks.
- Responsibility2: Data collection and analysis

Research Collaboration – *Prof. Yunjie Tong*   *Nov 2018 – Present*

- Project: Modeling of spatially-defined hemodynamic response function (HRF) using unsupervised clustering that can help the characterization of interaction between end-tidal CO_2 and BOLD-fMRI (e.g., analysis of cerebrovascular reactivity)
- Responsibility: Dimensionality reduction (i.e., PCA, t-SNE), Clustering (i.e., k-means), Optimization of parameters, Data collection, Pre-processing of fMRI and T1-weighted images

Research Collaboration – *Prof. Zhenhu Liang*   *Oct 2018 – Present*

- Project: Prediction of patients' status in anesthesia treatment during surgery using a single-channel EEG collected at multiple sites using different hardware and drugs. Classification among wakefulness, general anesthesia, burst suppression, and recovery of consciousness.
- Responsibility: Development of a neural network-based model that provides high prediction performance, Exploration of input/feature type (input to neural networks) – e.g., raw signal, entropy, spectrogram, response power spectral density. Keywords: CNN, LSTM, Transfer Learning

Data Analyst – *Dr. Bridget Walsh*   *Apr 2014 – Dec 2014*
- Project: Characterization and identification of brain signals of stuttering children compared to healthy controls using functional near-infrared spectroscopy (fNIRS).
- Responsibility: Signal processing and analysis of the fNIRS data.

Medical Imaging Laboratory (MILAB)   Seoul, South Korea
Pre-Doctoral Internship – *Prof. Dong-hyun Kim*   *Feb 2013 – Jul 2013*
- Project 1: Enhanced image reconstruction of electric conductivity from MRI
- Project 2: Total variation de-noising of MR images

Yonsei University   Seoul, South Korea
- (Undergrad thesis) Real-time head-mounted eye tracking system with compensation of   *Jul 2012 – Dec 2012*
  movements: implementation of hardware (using infrared cameras) and software (C++ & OpenCV)
  - *Prof. Sanghoon Lee*   *Mar 2012 – Jun 2012*
- (Short-term project) Partial *K*-space reconstruction of MRI (Matlab) – *Prof. Dong-hyun Kim*   *Jul 2011 – Sep 2011*
- (Undergrad SW intern) 3-D rendering from 2-D X-ray CT brain images (C++ & OpenGL) – Prof. Sanghoon Lee

Industry Experience

NVIDIA   Holmdel, NJ
- Deep Learning Intern on the Autonomous Driving R&D team   *May 2018 – Aug 2018*
- Projects (mostly with C++):
  1) Generate "extreme but physically possible" randomized trajectories based on recorded data/trajectories then apply viewport transform to the recorded videos to generate artificial videos. This data augmentation allows the self-driving cars to cope with unseen situations.
  2) Extend the current training architecture to add feedback connections using LSTM layers to memorize circumstances/features that may be important at an unknown time in the future and cope with unexpected situations.
  3) Re-implement and improve the neural network's data prep & training infrastructure to make it ready for rapid iterations with a massive amount of data.
- Other responsibilities: Algorithm enhancement, Data preprocessing, Interfacing with sensors, SW development (writing tests, code review, continuous integration, etc.)

Earlens (Startup)   Menlo Park, CA
- Research Intern on the Custom Products R&D team   *Jun 2016 – Aug 2016*
- Project (mostly with Matlab & Python): Analysis of hearing aids' alignment between photodetector and light tip emitter (which transmits power and signal) in the ear when patients talk, smile, or yawn, to estimate and optimize the performance and power efficiency of the system. The main experiment used three infrared cameras (for 3-D tracking) to estimate the location and angle of the device when subjects are in motion.
- Responsibilities:
  1) Computer Vision & Image Processing. e.g., edge and feature detection, point tracking, line fitting, rigid-body tracking, camera calibration, un-distortion using intrinsic parameters.
  2) 3-D Geometry Calculation. e.g., estimation of camera motion (translation and rotation) from consecutive 2-D images taken by a camera.
  3) Experimental design, Data collection, and Statistical analysis and data mining.
  4) Algorithm Automation. e.g., Matlab, Python, Grasshopper (3-D modeling/analysis tool).

Teaching Experience

Full-time Lecturer – Signals and Systems (ECE 301), Purdue University   West Lafayette, IN
- Topics: LTI system, Fourier series, Fourier transform, Sampling theory, Z-Transform, etc   *Jun 2016 – Aug 2016*
- Responsibility: Coordinating course with TA and grader, Lecturing, Development of exams, homework, and quizzes, Proctoring and grading exams, and Holding office hours.

Lab Instructor (Teaching assistant) – Digital Signal Processing (ECE 438), Purdue University   *Aug 2014 – Dec 2018*
- Worked with: Profs. Jan Allebach, Mireille Boutin, and Okan Ersoy
- Topics: Frequency analysis, Sampling and reconstruction, Interpolation and decimation,
  Waveform quantization, DFT and FFT, Digital filter design, Speech recognition and synthesis,
  Image processing, Halftoning, Random processes, etc.
- Responsibility: Instructing lab sessions, Lab development, Syllabus & Rubric development,
  Holding office hours, Grading reports, quizzes, and codes.

Mentoring undergraduate researchers – different projects for three students (all entered grad school)

Training graduate researchers – operate MRI and cognitive tests

---

Grants

1.	**GPU Seeding Grant –** NVIDIA Corporation; drafted research proposal	*May 30, 2017*
2.	**Trainee Stipend** – International Society for Magnetic Resonance in Medicine (ISMRM)	*Mar 01, 2019*
3.	**Travel Grant** – Purdue Graduate Student Government (PGSG)	*Nov 18, 2018*
4.	**Trainee Stipend** – ISMRM Workshop on Machine Learning, Part II.	*Sep 27, 2018*
5.	**Travel Grant** – Purdue Graduate Student Government (PGSG) – Top 10%	*Mar 14, 2018*
6.	**Scholarship** – International Congress on Magnetic Resonance Imaging (ICMRI)	*Feb 27, 2018*
7.	**Trainee Stipend** – Joint Annual Meeting ISMRM-ESMRMB	*Feb 15, 2018*
8.	**Trainee Stipend** – ISMRM Workshop on Advanced Neuro MR	*Feb 12, 2018*
9.	**Travel Grant** – Purdue Graduate Student Government (PGSG) – Top 10%	*Mar 15, 2017*
10.	**Travel Grant Award** – Purdue Institute for Integrative Neuroscience (PIIN) – 1st Place	*Mar 01, 2017*
11.	**Trainee Stipend** – International Society for Magnetic Resonance in Medicine (ISMRM)	*Feb 16, 2017*

Presentations

Platform Talks:

1. **Ikbeom Jang**, "Fluid Intelligence Prediction from T1-weighted MRI using a Multimodal Convolutional Neural Network," *The Purdue Association for Magnetic Resonance,* West Lafayette, IN, Feb. 2019. Invited Talk
2. **Ikbeom Jang**, "Automated Quality Assurance of Diffusion MR Images Using A Domain Transferred Deep Convolutional Neural Network," *ISMRM Workshop on Machine Learning,* Washington D.C., Oct. 2018
3. **Ikbeom Jang**, "Anomaly Detection from High School Football Players: Longitudinal DTI Study with a Large Cohort", *The 6th International Congress on Magnetic Resonance Imaging*, Seoul, South Korea, Mar. 2018. Best Poster Award
4. **Ikbeom Jang**, "Microstructural White Matter Changes in Asymptomatic Football Athletes: Longitudinal DTI Study", *ISMRM Workshop on Advanced Neuro MR: Best Practices for Technical Implementation*, Seoul, South Korea, Mar. 2018.
5. **Ikbeom Jang**, "What Can We Do with Statistics and Machine Learning in MRI?" *Purdue Association for Magnetic Resonance*, Purdue University, West Lafayette, IN, Jan. 2018. Invited Talk
6. **Ikbeom Jang**, "Deep Learning Applications in Computer Vision and Medicine", *Big Data Theory Seminar*, Purdue University, West Lafayette, IN, Dec. 2017. Invited Talk
7. **Ikbeom Jang**, "Stepwise Regression to Identify Predictors of Microstructural White Matter Abnormalities in Football Athletes", *The 5th Indiana Neuroimaging Symposium*, West Lafayette, IN, Nov. 2017. Selected as Best-5 Paper
8. **Ikbeom Jang**, "Healthcare-Integrated Automotive: The Car as a Healthcare Device", *2017 Hyundai Global Top Talent Forum*, San Diego, CA, Aug. 2017. Best Proposal Award
9. **Ikbeom Jang**, "Diffusion Tensor Imaging Reveals Persistent Effects on White Matter Microstructure in High School Football Players with History of Sports-Related Concussion," *25th ISMRM*, Honolulu, HI, Apr. 2017. Magna Cum Laude awarded
10. **Ikbeom Jang**, "DTI reveals persistent effects on white matter in football athletes with history of concussion," *The 4th Indiana Neuroimaging Symposium*, Bloomington, IN, Nov. 2016.

Selected Poster Presentations (among nine)**:**

1. **Ikbeom Jang**, Yukai Zou, and Thomas Talavage, "Automated Quality Assurance of Diffusion MR Images Using A Domain Transferred Deep Convolutional Neural Network," *ISMRM Workshop on Machine Learning,* Washington D.C., Oct. 2018

2. **Ikbeom Jang**, Victoria Poole… and Thomas Talavage, "Anomaly Detection from High School Football Players: Longitudinal DTI Study with a Large Cohort", *The 6th International Congress on Magnetic Resonance Imaging*, Seoul, South Korea, Mar. 2018.

3. **Ikbeom Jang**, Victoria Poole… and Thomas Talavage, "Using Machine Learning to Classify Youth Football Athletes with Accumulated Head Blows based on Diffusion MRI", The *5th Indiana Neuroimaging Symposium,* West Lafayette, IN, Nov. 2017.

Technical Skills

Programming Skills	Fluent: Python, C++, C, MATLAB, Linux Shell, R, STATA, Excel Intermediate: JAVA, Android, SQL
Deep Learning Frameworks	Tensorflow, Keras
MRI Analysis Tools	FSL, AFNI, DIPY
Patent	"UMBRELLA HAVING STANDING MEMBER", Republic of Korea, Reg. No.: 1009875800000, Oct 16, 2010
Certificates	Primary MRI Operator – *GE Discovery MR750 3.0T at Purdue MRI Facility* – *GE Signa HDx 3.0T at InnerVision Advanced Medical Imaging Center* Portable EEG Operator – *Brainscope Ahead® 200* Certificate of Information Processing – *Korea Testing Institute of Technical Qualification*
Graduate-Level Courses	(Offline) Statistical Machine Learning, Data Mining, Pattern Recognition & Decision Making Process, Big Data Theory, Medical Imaging & Diagnostic Techniques, Biostatistics, Optimization Methods for Systems & Control, Intro. to Mathematical Statistics, Digital Signal Processing, Digital Image Processing, Linear Algebra (Online) Convolutional Neural Networks for Visual Recognition (Stanford CS231n)

Awards and Honors

1. **Best Poster Award with Scholarship** – International Congress on Magnetic Resonance Imaging (ICMRI) — *Mar 31, 2018*
2. **Hyundai Motors Best Proposal Award** – Hyundai Motor Group — *Aug 19, 2017*
   - Title: Healthcare-Integrated Automotive: Car as a Healthcare Device
3. **Magna Cum Laude Merit Award** – International Society of Magnetic Resonance in Medicine — *May 11, 2017*
4. **LG Electronics Award for Outstanding Undergraduate Thesis** — *Nov 08, 2012*
   - Title: Robust Head-Mounted Eye Tracking System Allowing Head Movements
5. **Honors Student Awards (three times)** – Yonsei University — *2012 Fall, 2012 Spring, 2007 Spring*
6. **Honors Tutor Award** – Center for Teaching and Learning, Yonsei University — *Sep 03, 2012*
7. **Commendation Award** – Senator and Top-up Assembly Member, South Korea — *Feb 06, 2007*
8. **Commendation Award and Medal** – Governor of Gangnam-gu, Seoul, South Korea — *Oct 25, 2006*

Fellowships

National Science and Technology Fellowship – Korea Science and Engineering Foundation — *2007 - 2012*

Data Science Competitions

ABCD Neurocognitive Prediction Challenge (in conjunction w/ MICCAI 2019) – racing for Purdue150 team — *Jan 2019 – Apr 2019*

- Task: To develop a model for predicting fluid intelligence from T1-weighed MRI (8.5K subjects in total).
- Responsibility: Modeling of a multimodal 3-D CNN that takes 3-D T1w images, volumetric features, and demographic information
- Achievement: Ranked 8-th among ~150 registered teams (based on validation performance)

Citadel Datathon (by Citadel and Citadel Securities) – raced for Purdue team

Chicago, IL, US
May 12, 2017

- Task: To analyze how development of U.S. labor market post-financial crisis relate to broader economic and financial trends since 2007. Use machine learning or time series analysis to predict future job postings trends.
- Responsibility: Prediction using Autoregressive integrated moving average (ARIMA) and Support vector machine.

PUBLICATIONS

PUBLICATIONS

Ikbeom Jang et al., "Every Hit Matters: White Matter Integrity Changes in High School Football Athletes Are Correlated with Recent Repetitive Head Acceleration Event Exposure," In revision in Neuroimage: Clinical, 2019

Ikbeom Jang et al., "Low-Magnitude Hits Matter: Single-Season Longitudinal DTI Study on Asymptomatic High School Football Players," Proc. Intl. Soc. Mag. Res. Med. (ISMRM), Montreal, Canada, May. 2019

Ikbeom Jang et al., "Long-term Changes in White Matter after Sports-Related Repetitive Head Impacts: An Across-Season DTI Study." Journal of Neurotrauma, vol. 35, no. 16, pp. A116, 2018

Ikbeom Jang et al., Automated Quality Assurance of Diffusion MR Images Using A Domain Transferred Deep Convolutional Neural Network, Intl. Soc. Mag. Res. Med. (ISMRM) workshop on Machine Learning, Washington D.C., MD, 2018.

Ikbeom Jang et al., "Test-Retest and Between-Site Reliability in a Multisite Diffusion Tensor Imaging Study," Proc. Intl. Soc. Mag. Res. Med. (ISMRM), Paris, France, Jun. 2018

Ikbeom Jang et al., Anomaly Detection from High School Football Players: Longitudinal DTI Study with a Large Cohort, The 6th International Congress on Magnetic Resonance Imaging (ICMRI), Seoul, South Korea, Mar. 2018.

Ikbeom Jang et al., Microstructural White Matter Changes in Asymptomatic Football Athletes: Longitudinal DTI Study, ISMRM Workshop on Advanced Neuro MR: Best Practices for Technical Implementation, Seoul, South Korea, Mar. 2018.

Ikbeom Jang et al, "Machine Learning based Classification using Diffusion Tensor MR Imaging to Detect Youth Athletes with Repetitive Head Blows," Biomedical Engineering Society (BMES), Phoenix, Arizona, Oct. 2017.

Ikbeom Jang et al., "Group-level White Matter Analysis for Middle School Football Athletes in Comparison with High School Athletes: DWI Study," Biomedical Engineering Society (BMES), Phoenix, Arizona, Oct. 2017.

Ikbeom Jang et al., "Predictor Identification for White Matter Integrity in Football Athletes using Stepwise Regression," Proc. Org. for Hum. Brain Mapp. (OHBM), Vancouver, Canada, Jun. 2017.

Ikbeom Jang et al., "Diffusion Tensor Imaging Reveals Persistent Effects on White Matter Microstructure in High School Football Players with History of Sports-Related Concussion," Proc. Intl. Soc. Mag. Res. Med. (ISMRM), 2017

Ikbeom Jang et al., "Collision-Sports and Axonal Impairment: DWI Assessment in High School Football Athletes," Proc. Org. for Hum. Brain Mapp. (OHBM), Geneva, Switzerland, 2016.

Ikbeom Jang et al., "DWI Detection of WM Abnormality and Relation with Collision Events in High School Athletes," Proc. Org. for Hum. Brain Mapp. (OHBM), Honolulu, HI, 2015.

Ikbeom Jang et al., "Robust Detection of Axonal Abnormalities in High School Collision-Sport Athletes: Longitudinal Single Subject Analysis," Proc. Intl. Soc. Mag. Res. Med. (ISMRM), Toronto, ON, 2015.

Sumra Bari, Diana O. Svaldi, Ikbeom Jang, et al., "Dependence on subconcussive impacts of brain metabolism in collision sport athletes: an MR spectroscopic study." Brain imaging and behavior (2018): 1-15.

Yukai Zou, Taylor Lee, Roy J. Lycke, Ikbeom Jang, et al., "High-G Head Collisions are Associated with Short-Term White Matter Microstructural Deficits in High School Football Athletes." Journal of Neurotrauma, vol. 35, no. 16, pp. A23, 2018

Yukai Zou, Ikbeom Jang, et al., "Prediction of white matter microstructural maturation in adolescent American Football athletes using history of sport-participation and concussion," Proc. Intl. Soc. Mag. Res. Med. (ISMRM), Paris, France, Jun. 2018

Yukai Zou, Ikbeom Jang, et al., "Acute Impacts of Football Competition on Brain White Matter Microstructure in High School Athletes," Biomedical Engineering Society (BMES), Phoenix, Arizona, 2017.

Yukai Zou, Ikbeom Jang, et al., "Abnormal White Matter Microstructure and Cognitions in Adolescent Athletes with Concussion History," Biomedical Engineering Society (BMES), Phoenix, Arizona, 2017.

MacKenzie Tweardy, Ikbeom Jang, et al., "Volumetric White Matter Changes due to Accumulated Subconcussive Impacts in Football and a Traumatic Car Accident," Biomedical Engineering Society (BMES), Phoenix, Arizona, 2017.

Yukai Zou, Xianglun Mao, Ikbeom Jang, et al., "Short and Long-term White Matter Microstructural Differences in Adolescent Female Soccer Athletes," Biomedical Engineering Society (BMES), Phoenix, Arizona, 2017.

Sumra Bari, Kausar Abbas, Ikbeom Jang, et al., "Multi-site reliability of resting state fMRI using graph theoretical measures," Proc. Org. for Hum. Brain Mapp. (OHBM), Vancouver, Canada, 2017.

Yukai Zou, Ikbeom Jang, et al., White matter microstructure in previously concussed adolescent athletes: implications on cognition, Proc. Org. for Hum. Brain Mapp. (OHBM), Vancouver, Canada, 2017.

Pratik Kashyap, Ikbeom Jang, et al., "Resting state functional connectivity alteration in asymptomatic high-school female soccer athletes," Proc. Org. for Hum. Brain Mapp. (OHBM), Vancouver, Canada, 2017.

Yukai Zou, Xianglun Mao, Ikbeom Jang, et al., "White matter microstructure in adolescent female soccer athletes: diffusion MRI relations with years of high-school experience, concussion history, and cognitive measurements," Proc. Intl. Soc. Mag. Res. Med. (ISMRM), 2017.